THE PENNSYLVANIA STATE UNIVERSITY
SCHREYER HONORS COLLEGE

DIVISION OF SCIENCE

BINDING AFFINITIES OF FLAVINS TO RIBOFLAVIN BINDING PROTEIN USING FLUORESCENCE SPECTROMETRY AND ISOTHERMAL TITRATION CALORIMETRY, AND ESTIMATED BINDING ENERGIES USING COMPUTATIONAL APPROACHES

HABIB YAZGI
SPRING 2018

A thesis
submitted in partial fulfillment
of the requirements
for a baccalaureate degree
in Biology
with honors in Biology

Reviewed and approved* by the following:

Julie Ealy
Associate Professor of Chemistry
Thesis Supervisor

Sandy Feinstein
Associate Professor of English
Honors Adviser

* Signatures are on file in the Schreyer Honors College.

ABSTRACT

Riboflavin binding protein is specific for transporting riboflavin from the human mother to the fetus during pregnancy. This protein is a highly conserved protein and is found in different species, which supports its importance in sustaining the development of the fetus. Elevation of riboflavin binding protein (RBP) has been associated with breast cancer in women. This elevation suggests that it might be a good biomarker to detect early breast cancer. Recently, riboflavin binding protein (RBP) antisera has been observed to cause riboflavin depletion in the human cervical cancer cell line (HeLa). This observation suggests that RBP can be a point of intervention for therapeutic drugs against cancer.

Modern drug development techniques are attempting to rely more on computational approaches to measure the binding affinity of ligand-protein interactions and these approaches will save time and money. However, computational programs do not always account for all the ligand-protein interactions that contribute to binding affinity. This failure can contribute to discrepancies between wet bench lab techniques and a computational approach. Thus, we assessed how ICM-Pro (computational software) and fluorescence spectrometry performed in the determination of the binding affinity of riboflavin, lumichrome, FMN, and FAD. These results were compared to the established method (isothermal calorimetry titration (ITC)). ITC and fluorescence spectrometry used RBP, but ICM-Pro used human folate receptor alpha (4LRH.pdb), which is an evolutionarily related protein to RBP. Human folate receptor alpha protein has also been implicated in cancer, and researchers have been striving to develop new cancer drugs for this protein. For that reason, we also have compared 4LRH.pdb to RBP sequences and structures to each other. These results will potentially provide novel insights into

these two proteins that can be utilized for potential cancer drug development for RBP as well as human folate receptor alpha.

We have found that ICM-Pro results did not match the results from ITC, perhaps because two different proteins were used. However, future work is needed to verify these results. Fluorescence spectrometry results had consistent difference values compared to the ITC results. These differences suggest that the less expensive fluorescence spectrometry could be used to measure accurate binding affinities. However, testing more flavins is needed to verify the consistency of these differences between fluorescence spectrometry and ITC. Structural analysis of RBP and human folate receptor alpha demonstrated a significant similarity between the two proteins thus indicating their similar functions.

Riboflavin was shown to have almost identical positions in both proteins with respect to Tyr75 and Trp156 in RBP and their corresponding amino acids Tyr85 and Trp171, respectively, in human folate. The distance between riboflavin and the two amino acids was almost identical in both proteins. The structural analysis of the position of riboflavin in 4LRH.pdb and RBP and the measurement of the flavins' binding affinities using ITC, ICM-Pro and fluorescence spectrometry provide information on the similarities and differences between these two proteins.

This research also provides avenues for further structural investigation of drug-like and nondrug-like flavin molecules in 4LRH.pdb and their relationship to the estimated binding energies using ICM-Pro. This will further enhance our understanding of the relationship between RBP and human folate receptor alpha and provide new opportunities for future cancer drug development.

TABLE OF CONTENTS

LIST OF FIGURES

LIST OF TABLES

ACKNOWLEDGMENTS

I would like to thank my Thesis Supervisor, Dr. Julie Ealy, Associate Professor of Chemistry at Penn State Lehigh Valley, for sponsoring me for the completion of my thesis in her laboratory and giving me continuous instructions and invaluable advice for the last three years. I would also like to thank the Honors Adviser, Dr. Sandy Feinstein at Penn State Berks for her feedback and constructive comments during my thesis development. Noorhan Abouomar has participated in this research from the beginning. Thank you for your time and the effort you put into this research. I would also like to thank The Huck Institutes of the Life Sciences at Penn State UP for their monetary support to perform the isothermal calorimetry experiments and specifically Julia Fecko and Dr. Neela Yennawar for performing the experiments and supporting us with the necessary technical knowledge. Thank you, Mrs. Pam Borowski at Penn State Leigh Valley for ordering the necessary chemicals and laboratory supplies. I also want to thank Melissa Hill at Vernier.com for answering our questions about fluorescence spectrometry. Thank you, also, to Adam Shapiro at Entasis Theraputics for answering many questions about binding affinity.

Thank you to my parents, Ayman Yazgi and Suhir Almalouli, for encouraging my love of science and providing for me so I could attend Penn State. I would not be here without you.

.

Chapter 1

Introduction

Riboflavin is vitamin B2 (7, 8-dimethyl-10-ribityl-isoalloxazine) and is a water soluble vitamin present in a wide variety of foods (Powers, 2003). Riboflavin participates in a variety of different redox reactions that are essential to human metabolism. Those reactions occur using the active forms of riboflavin, cofactors flavin mononucleotide (FMN) and flavin adenine dinucleotide (FAD) that act as electron carriers (McCormick et al., 1988). Riboflavin deficiency has been linked to diverse abnormalities in mice and rats (Warkany and Nelson, 1942), anemia in humans (Foy and Kondi, 1953), and mental illness (Bell et al., 1992).

As a micronutrient, riboflavin is transported in the plasma, and it is often bound to plasma proteins such as albumin, certain immunoglobulins, and riboflavin binding protein (Innis et al., 1985). This ensures and facilitates the delivery of the riboflavin to the tissues and prevents it from being filtered through the kidney (Merrill et al., 1982).

Riboflavin binding protein is a protein that is specific for transporting riboflavin from the human mother to the fetus during pregnancy (Visweswariah and Adiga, 1987a). This protein is expressed in different species' fetuses, and is important in sustaining the embryological development of the fetus (Natraj et al., 1987; Murty and Adiga, 1981). During pregnancy, the riboflavin concentration of the human cord serum is four times that of the maternal serum (Clarke, 1977). As a water-soluble vitamin, riboflavin cannot cross the placenta membranes because the placenta is relatively impermeable to free riboflavin (Dancis, 1962). Some suggest

that there is a specific carrier-mediated transport system (Natraj et al., 1988) for riboflavin. The human species also uses a specific type of riboflavin binding protein that is unique to pregnancy and that transports riboflavin properly to the fetus.

Studies have also shown that riboflavin binding protein is important in the chicken egg, is stimulated by estrogen, and is critical for the survival of the fetus (White III and Merrill, 1988). A study by Natraj et al. (1988) showed that the umbilical cord serum contains a protein that is different from serum albumin, and this riboflavin binding protein inside the umbilical cord was closely similar in molecular weight and function to its chicken counterpart. This research suggests that riboflavin binding proteins are highly conserved (Natraj et al., 1988).

Elevation of riboflavin binding protein (RBP) has been associated with breast cancer in women (Rao et al., 1999). The association of RBP with breast cancer suggests it might be a good biomarker to detect early breast cancer (Karande et al., 2001). Riboflavin binding protein (RBP) antisera has also been observed to cause riboflavin depletion in the human cervical cancer cell line (HeLa) (Kudle et al., 2017).

This research is the first attempt to compare computationally estimated binding energies of flavins docked into human folate receptor alpha with binding affinities of the same flavins with riboflavin binding protein (RBP). Both proteins are carriers that bind to different types of vitamin B; RBP carrying vitamin B2 (riboflavin) and human folate receptor alpha carrying vitamin B9 (folic acid). Both of these evolutionarily related carriers were found to be expressed in tumor cells.

Through this comparison, our research assesses how close computational estimated binding energy values are to those of ITC and fluorescence spectrometry in measuring the tightness of binding of the flavins to the two related proteins. Furthermore, we computationally

investigate the intermolecular interactions between riboflavin and human folate receptor alpha. These interactions are compared to published investigations of intermolecular interactions between riboflavin and RBP. This comparison will allow us to further assess how the evolutionarily related proteins interact with riboflavin that represents the basic structure of flavins. Amino acid sequences of human folate receptor alpha are also compared with RBP amino acid sequences to further investigate the evolutionary closeness of both proteins. The investigation of the sequences of the two proteins and their intermolecular interactions with riboflavin will give us a better picture of how close the active sites of both proteins are to each other. Combined with in silico and in vitro results, the structural and computational investigation assesses whether human folate receptor alpha is a good computational model to represent RBP.

Additionally, we compare how close fluorescence spectrometry is to isothermal calorimetry titration (ITC) in measuring the binding affinities of four flavins to RBP. ITC is one of the most accurate methods for measuring ligand-protein binding affinities and comparing fluorescence spectrometry to it will allow us to see whether this method can be used as an accurate method in measuring binding affinities.

Since both proteins, RBP and human folate receptor alpha, have been found to be expressed in tumor cells, our investigation about their active sites provides insights into the structural interaction of the flavins with human folate receptor alpha. Our experiments in measuring the tightness of binding of the four flavins to these proteins computationally and experimentally could provide a template for future drug development as it relates to riboflavin and riboflavin binding protein.

Chapter 2

Literature Review

Nomenclature

Riboflavin binding protein has many names and abbreviations that can be confusing. Some papers refer to it as riboflavin binding protein (RBP (White III, 1987), others call it riboflavin receptor protein (RCP) (Zak et al., 1972), and still others call it riboflavin-flavoprotein (Zak and Ostrowski, 1963). Here, we refer to it as riboflavin binding protein (RBP).

Structure of Riboflavin Binding Protein (RBP)

Egg white riboflavin binding protein (RBP) is a protein comprised of 219 amino acids (Hamazume et al., 1984). RBP is a globular monomeric protein of the approximate dimensions, 50 x 40 x 35 Å with a cleft approximately 20 Å wide and 15 Å deep that is the vitamin binding site (Monaco, 1997). The protein consists of two distinctive major regions. The first one is the ligand-binding domain that begins with Glu1 at the N-terminus, and extends to Cys 169 at the C-terminus. The second domain extends from Leu 170 at the N-terminus to Glu 219 at the C-terminus (Monaco, 1997). The entire protein is composed of six α-helices, that include 30 % of the total residues and four nonconsecutive areas of β structures that comprise a little less than 15 % of the protein. The ligand-binding domain has 4 α-helices, and 4 β structures that are separated by loops of amino acids. In the second domain there are mainly two α-helices separated by a phosphorylated region that is not well ordered (Monaco, 1997). The phosphorylated region connects the last two α-helices from Glu 186 to Glu 199; it is highly anionic because glutamic

acid comprises most of it (Hamazume et al., 1984). The phosphorylation in this region occurs on the serine amino acids to form phosphoserine. The serines were determined to be S187, S188, S191, S192, S193, S195, S196, and S197 (Hamazume et al., 1984).

Dephosphorylating the RBP in chicken blood plasma reduces its reuptake into the oocyte significantly (Miller et al., 1982a). This finding indicates that this phosphorylated region is important in the recognition of the plasma RBP by the oocyte receptor. The last two helices in the protein that are connected by an anionic region were found to be on the outside of the protein. The anionic region protrudes into the solvent and provides structural evidence for its function (Monaco, 1997). RBP has oligosaccharides attached to it with two attached to Asn 36 and Asn 147 (Hamazume et al., 1984). Egg white RBP (Norioka et al., 1985), yolk, and serum RBP have different carbohydrate compositions. They all have complex glycoproteins that have twice as many N-acetylglucosamine residues as mannose. However, egg white RBP is different from yolk and serum RBP in that it has only one sialic acid and two galactose residues (Miller et al., 1982b). Egg white RBP has nine disulfide bonds between different cysteines along its amino acids sequence. The disulfide bonds in bold 8*, and 9* were reported to be alternative disulfide bonds of cysteines 8 and 9 (Hamazume et al., 1987).

Table 2.1: RBP disulfide bonds

Disulfide bond (DS)	1st Residue		2nd Residue	
DS1	(Coil)	*Cys (24)*	*Cys(73)*	(Helix)
DS2	(Coil)	*Cys (57)*	*Cys(138)*	(Coil)
DS3	(Helix)	*Cys(64)*	*Cys(l 10)*	(Helix)
DS4	(Strand)	*Cys(99)*	*Cys(169)*	(Coil)
DS5	(Coil)	*Cys(116)*	*Cys(134)*	(Strand)
DS6	(Helix)	*Cys(103)*	*Cys(152)*	(Helix)
DS7	(Coil)	*Cys(167)*	*Cys(202)*	(Helix)
DS8	(Coil)	*Cys(5)*	*Cys(32)*	(Coil)
DS9	(Coil)	*Cys(33)*	*Cys(77)*	(Helix)
DS8*	**(Coil)**	***Cys(5)***	***Cys(33)***	**(Coil)**
DS9*	**(Coil)**	***Cys(32)***	***Cys(77)***	**(Helix)**

RBP disulfide bonds. The nine disulfide bonds of RBP and the position of each of cysteine in sequence and in the crystal structure.

RBP-riboflavin Complex

Riboflavin binds to riboflavin binding protein in the ligand-binding domain cleft that is ~20 Å wide and 15 Å deep (Monaco, 1997). The riboflavin binding occurs in the cleft where its isoalloxazine ring is stacked between the planes of two amino acids, Tyr75 and Trp156. The ring is composed of pyrimidine and xylene moieties with either one responsible for the binding. To determine which of the two moieties is most important for binding, research (Merrill and

Mccormick, 1978) showed that altering the flavins at the N (3) position in the pyrimidine moiety had almost no effect. It showed that when this position was altered there was no hindrance when binding to the apo egg white RBP. Regarding the xylene aromatic ring moiety, several studies showed that it had significant importance in the interactions between flavins and RBP. Mifflin and Langerman (1983) found that through changes in binding free energy values, there were ligand steric interactions in the areas of C7, C8, and C9 of the xylene aromatic ring moiety. The electron density of vitamin B2 (riboflavin) inside the active site of RBP shows that the xylene moiety is deeply buried inside the molecule and the major interactions between the ligand and RBP are hydrophobic (Monaco, 1997). The electron density map was similar to previously published studies that showed when the riboflavin structure was altered the binding energy changes from the RBP-riboflavin interactions were mostly hydrophobic.

Function

There is a considerable increase in concentration of riboflavin in the serum of the laying hen; it is substantially higher than in males and non-laying hens (Common et al., 1946). In addition, the administration of estrogen to an immature pullet (immature female chicken) resulted in about a 100-fold increase in serum riboflavin (Bolton, 1950). Research showed that riboflavin deficiency causes a large increase in hemorrhagic embryos (Squires and Naber, 1992), and this supports the significant role of riboflavin in early development (Goldsmith, 1975; Squires & Naber, 1992).

In the human blood serum, a major fraction of riboflavin is transported by a protein known as albumin (Jusko and Levy, 1969). Similar to albumin, some immunoglobulins were

found to bind to riboflavin as carriers. For example, riboflavin binding by IgG and IgA was demonstrated using immunoelectrophoresis (Innis et al., 1985).

A unique carrier protein called riboflavin binding protein (RBP) has been discovered in a chicken disease called ribonavinuria (Hammer et al., 1973). Chickens that had ribonavinuria were found to be homozygous recessive for the *rdrd* gene, and lost their embryos because of premature death (Hammer et al., 1973; Winter et al., 1967). Because they were recessive for the *rdrd* gene, these chickens could not produce riboflavin binding protein (RBP) (White et al., 1992). Research has also found that chickens that lacked RBP had higher than usual levels of riboflavin excreted in their urine (Cowan et al., 1966). This observation further supports the argument that the absence of RBP in chickens with ribonavinuria disables the transportation of riboflavin to the embryos that leads to their death. The death of the embryos, however, did not affect the mothers and indicated that riboflavin metabolism is not impaired, which confirmed the role of RBP in transporting riboflavin to the fetus (White et al., 1992).

The vitamin-protein complex and apoprotein, if present, are deposited in the yolk of developing oocytes (Zak and Ostrowski, 1963). RBP is produced by the oviduct in response to estrogen (DurgaKumari and Adiga, 1986), and then it is secreted as part of the egg albumen (egg white) (Rhodes et al., 1959). RBP is also produced in the liver in response to estrogen (Murthy and Adiga, 1978a) and is then secreted into the blood plasma where it binds to riboflavin. Riboflavin carrier protein has been purified from three different sites in chickens: yolk (Murthy et al., 1979), egg-white (Rhodes et al., 1959), and serum (Murthy and Adiga, 1978b). The three forms have some minor differences in their structural features, most likely attributed to post-translational modifications (Narioka et al., 1985).

The importance of RBP in pregnancy is apparent in other animals, most notably mammals. For example, antibodies for chicken RBP were administered to terminate pregnancy in mice with well-formed placentas (Natraj et al., 1987). Because of the homology between mice RBP and chickens RBP, pregnancy was successfully terminated in mice using chicken RBP antibodies. Another study on rats confirmed the role of the RBP system in rats by termination of their pregnancies with chicken RBP antibodies (Murty and Adiga, 1981)

Isolated RBP from primates, bonnet monkeys, was similar to its avian counterpart in many ways such as isoelectric point, electrophoretic mobility, molecular weight, and ligand binding (Visweswariah and Adiga, 1987b). RBP was also shown to be present in human pregnancy and umbilical cord sera exhibiting a remarkable immunological cross-reactivity with the RBP isolated from the chicken egg (Visweswariah and Adiga, 1987a). This RBP was similar to chicken RBP in many aspects such as isoelectric point (4.1), molecular weight (36,000 ± 2,000 Dalton), and preferential binding to free riboflavin (Visweswariah and Adiga, 1987a; Natraj et al., 1988).

The system of moving riboflavin from the human mother to the fetus has been shown to be dependent on RBP. First, riboflavin was detected in the amniotic fluid despite the relative impermeability of the placental membranes to riboflavin (Dancis, 1962). In addition, the cord serum was found to have four times the riboflavin concentration as maternal serum (Clarke, 1977). Clarke's finding was not consistent with the hypothesis of riboflavin simple diffusion to the fetus. The observation of riboflavin diffusion might indicate that riboflavin is transported by a mediated system, such as a carrier system, i.e, RBP (Dancis *et al.*, 1985).

RBP has been detected in amniotic fluid as well as in maternal and umbilical cord serum, and has shown significant cross reactivity with chicken RBP (Subramanian and Adiga, 1999).

Furthermore (Mason *et al.*, 2006), RBP has demonstrated involvement in riboflavin internalization. It has also been shown that when applying chicken RBP antibodies, the cellular riboflavin uptake is significantly decreased in human placental trophoblast (BeWo) cells (Mason *et al.*, 2006).

Detectable levels of human RBP were measured only after 4 months of gestation and remained high up to 8 months (Natraj et al., 1988). These results by Natraj et al. (1988) means that estimating the levels of RBP in maternal circulation can be important in order to monitor the progress of pregnancy, especially in high risk pregnancies. It has been noted (Murty and Adiga, 1982) that estrogen controlled the levels of RBP and, therefore, it is suggested that human RBP might be under the control of estrogen as well.

Sequence and Composition

RBP has 219 amino acids, as determined by Hamazume et al., 1984. The sequence matches the cDNA clone nucleotide sequence (Zheng et al., 1988). However, there is an additional 17-amino acid signal peptide from the N-terminus that is predicted by the nucleotide sequence. Also, from the C- terminus there are two adjacent arginine residues predicted by the nucleotide sequence but not present in the mature protein (Zheng et al., 1988). Hamazume *et al.* (1984) identified the first amino acid as pyroglutamate, which is not what the cDNA sequence predicts (Zheng et al., 1988). Perhaps this is because the cleavage site of a 17-amino acid signal peptide precedes the two neighboring glutamine residues (Zheng et al., 1988). The cleavage site involves the amino-terminal glutamine that cyclizes and eliminates ammonia, leaving the pyroglutamate that is found in the mature protein (Zheng et al., 1988).

There are two complex oligosaccharides attached to ASP 36 and ASP147 (Hamazume et al., 1984). Nine disulfide bonds have been identified in the mature protein, and they significantly contribute to the protein's tertiary structure and stability (Hamazume et al., 1987). There are phosphorylated serine residues close to the C-terminus. Three serine residues are phosphorylated: Ser (195), Ser (196), and Ser (197). However, the other six, Ser (185) to Ser (193), seem to be partially phosphorylated (Hamazume et al., 1984).

The sequence of hen egg-white riboflavin binding protein (RBP) is identical to plasma RBP and yolk RBP, except that the yolk lacks 11 or 13 amino acid residues from the C-terminal end (Norioka et al., 1985). The similarity suggests that all three RBP types are products of the same gene. The polymorphism at the fourteenth residue from the N-terminal end (Lys/Asn) (Hamazume et al., 1984) exists in egg-white, yolk, and plasma RBP (Norioka et al., 1985). Additionally, two Asn-linked glycosylation sites found in chicken RBP at Asn36 and Asn147, the phosphoserine rich C-terminal side and the pyroglutamate at the beginning of the N-terminal side, are shared characteristics among the three RBP types (Norioka et al., 1985). However, the composition of these carbohydrates in egg-white and yolk was noted to be different (Hamazume et al., 1984). Interestingly, the plasma and yolk RBP have the same sugar compositions, corresponding to those of complex type sugar chains (biantenna or triantenna), and egg-white RBP has an ovomucoid type structure (Yamashita et al., 1983; Hamazume et al., 1984; Norioka et al., 1985). The missing 11-13 residues and the composition of the carbohydrates indicate that the serum RBP is modified before or after it is included in the yolk (Norioka et al., 1985).

To illustrate the importance of the phosphorylation of the protein (Miller et al., 1982a), it was reported that the removal of a few phosphate residues drastically reduce the uptake of RBP into the oocyte. In other research, it was reported that the removal of sialic acid also reduced the

rate of incorporation (Miller et al., 1981). Thus, the phosphorylated region and the carbohydrates have been shown to have a role in the uptake of the RBP into the oocyte.

The isoelectric point of RBP is about 3.9-4.1 (Rhodes et al., 1959). The molecular weight of RBP, based on the amino acid, carbohydrate, and phosphoric acid composition, was reported as 29,200 $g \cdot mole^{-1}$ (Hamazume et al., 1984). However, this molecular weight value is less than the value recorded by SDS polyacrylamide gel-electrophoresis, which is 34,000 $g \cdot mole^{-1}$ (Hamazume et al., 1984), ultracentrifuge, 36000 $g \cdot mole^{-1}$ (Rhodes et al., 1959), and Sephadex G-100 chromatography, 37,000 $g \cdot mole^{-1}$ (Froehlich et al., 1980).

Folate

Folate receptors (FRα, FRβ and FRγ) are cysteine-rich cell-surface glycoproteins that bind folate with high affinity to mediate cellular uptake of folate (Chen et al., 2013). Folates (vitamin B9) are important carbon donors for the synthesis of nucleic acids and DNA methylation (Bailey and Gregory III, 1999). Folate deficiency has been connected with diseases such as neural tube defects (Stover, 2004). Folate receptors, especially FRα, are expressed at high levels in numerous cancers to meet the folate demand of the cancerous cells (Kelemen, 2006; Kane et al., 1988). A crystal structure of human folate receptor alpha (HFRA) is deposited in the Protein Data Bank (PDB) and is designated as 4LRH.pdb (Chen et al., 2013). Human folate receptor alpha, 4LRH.pbb, can be used to study the structure of the protein.

Binding Affinity

To investigate the binding of two molecules such as a ligand and a protein, understanding the interactions between the protein and its ligand is important. The ligand can be a drug, molecule, or a substrate with a protein or DNA or RNA. A ligand can bind to a macromolecule by ionic interactions and weaker intermolecular forces such hydrogen bonding and hydrophobic interactions. Because of the weakness of binding interactions, some of the complexes will dissociate to form a mixture of bound and unbound molecules. The strength of the molecular interaction between these molecules can be calculated by measuring the concentration of the free and associated species at equilibrium, and this strength is called the binding affinity (Kuriyan et al., 2009). The measurements of binding affinity are quantitative in that the number expresses how tightly the species bind together. There are two generic premises to measure the binding affinity: the reaction must be at equilibrium at the time of measurement and the concentration of one reactant must be varied (Pollard, 2010).

The generic binding equilibrium between a protein (*P*) and a ligand (*L*) represents the protein-ligand complex (PL) and is represented by equation [2.1]:

$$P + L <=> P\,L \qquad [2.1]$$

The equilibrium constant (K), i.e., the association constant (K_a), for reaction [1], is shown in equation [2.2] where [*PL*] is the concentration of the ligand- protein complex, [*P*] is the concentration of free protein, and [*L*] is the concentration of free ligand:

$$K_a = K = \frac{[P\,L]}{[P][L]} \qquad [2.2]$$

However, it is common to characterize the binding reaction (binding affinity) in terms of the equilibrium constant for the dissociation constant (K_d) rather than the association constant

(K_a). The dissociation constant (K_d) is the inverse of the association constant (K_a) as shown in equation [2.3]:

$$K_d = \frac{[P][L]}{[P\,L]} = \frac{1}{Ka} \qquad [2.3]$$

The value of K_d is equal in magnitude to the concentration of ligand at which half the protein molecules are bound to ligand (Kuriyan et al., 2009). The lower the K_d value, the tighter the binding affinity between the protein and ligand, and vice versa (Pollard, 2010).

Binding Energy

Molecular simulation can be defined as the numerical determination of the thermodynamic, energetic, structural, and dynamical properties of a mathematical model of a molecular assembly on a digital computer (Beveridge and DiCapua, 1989). Investigation of the dynamics of a protein's structural fluctuations and their relation to activity and conformational change is essential to understand their function (Karplus and Kurplus, 1983). Understanding the binding between the protein and ligand is important when it comes to rationalizing how cellular systems integrate and respond to molecular cues (Gallicchio and Levy, 2011). Measuring the tightness of the protein-ligand binding has many implications in medicine, especially in drug development (Jorgensen, 2004).

Two of the most commonly applied models for protein-ligand binding free energy estimation are molecular dynamics (MD) and Monte Carlo (MC)-based conformational sampling methods (Gallicchio and Levy, 2011). ICM (Internal Coordinate Mechanics) (Arnautova et al., 2011) is a simulation method that uses an improved (Monte Carlo) MC method to predict protein structure, homology modeling, molecular docking, nuclear magnetic resonance (NMR) structure

determination, and protein design (Abagyan et al., 1994). The program that was used in this research is called ICM-Pro that was developed to use ICM to conduct molecular simulations. These molecular simulations aim to estimate the binding energy of a ligand when it binds to a protein. The estimated binding energy (ΔG^0) can be converted to the dissociation constant (K_d) (binding affinity) using equation [2.4] (Kuriyan et al., 2009):

$$\Delta G^0_{bind} = RT \ln K_d \qquad [2.4]$$

Riboflavin and Cancer

Riboflavin's effects on cancer have been investigated since the mid twentieth century. Morris & Robertson (1943) showed that mammary tumor growth decreased in riboflavin deficient mice more than in mice that were not deficient in riboflavin (Morris & Robertson, 1943). Feeding supplemental vitamin B2 (riboflavin) to riboflavin deficient mice that had mammary cancer increased the growth of their cancer (Morris, & Robertson, 1943). Riboflavin deficient mice had smaller size tumors than mice that were not deficient in riboflavin (Morris, 1947). These studies suggest that riboflavin aggravated cancer growth in mice.

Breast cancer progression led to a significant decrease in the concentration of riboflavin in the serum (Vaidya et al., 1998) suggesting that cancerous cells consume more riboflavin than non-cancerous cells. At high concentrations, riboflavin was shown to increase lung cancer invasion and metastasis (Yang et al., 2013). However, at low concentrations, riboflavin did not cause any significant progression of non-small cell lung cancer (NSCLC) (Yang et al., 2013). In another study, FAD (flavin adenine dinucleotide) levels were significantly lower in NSCLC

patients compared to a control group (Tsao et al., 2007), suggesting that cancer cells consume more FAD, which is a derivative of riboflavin (Yang et al., 2013).

Furthermore, riboflavin treatment with UVA1 irradiation caused more DNA damage in the genome and, thus, it was responsible for oxidative DNA damage leading to mutagenesis in mouse embryonic fibroblasts (Besaratinia et al., 2007). The increase in the intake of riboflavin has been associated with increased gastric cancer risk as well (Kaaks et al., 1998).

Riboflavin deficiency has been shown to enhance the risk of esophageal cancer (EC) (Siassi and Ghadirian, 2005). In other research, vitamin B-6 and riboflavin intakes from diet and supplements were associated with a decreased risk of colorectal cancer (CRC) in postmenopausal women (Zschäbitz, et al., 2013).

Riboflavin Binding Protein (RBP) and Cancer

It has been found that riboflavin binding protein (RBP) was expressed in an elevated way in women with breast cancer (Rao et al., 1999). RBP has been found to be secreted with milk in response to estrogen and progesterone (Adiga et al., 1991). Studies have also shown an association between sex hormones (estrogen) and breast cancer (Zhang et al., 2013). Significantly, increased levels of serum RBP were highly predictive of breast cancer, detecting 88 % of tumors in stages I-II and 100 % of tumors in stages III-IV (Rao et al., 1999). This aspect of RBP could possibly be used as a biochemical marker to detect early breast cancer (Karande et al., 2001).

In addition, RBP was found to be localized in more than 95 % of androgen-insensitive PC3 cells grown in culture (Johnson et al., 2009). The protein (RBP) localization in the

cytoplasm of these cancer cells is similar to the localization of RBP reported in breast cancer tissues (Karande et al., 2001). Also, RBP has been shown to be elevated in hepatocellular carcinoma (Rao et al., 2006). Furthermore, RBP expression was also seen in androgen sensitive LNCaP as well as androgen insensitive PC3 and DU-145 prostate cancer cell lines (Johnson et al., 2009). Johnson's (2009) research showed that RBP expression in cancer cells can also be uncoupled from hormonal regulation (Johnson et al., 2009). Additionally, Johnson observed that antibodies for chicken RBP almost completely inhibited 3H riboflavin uptake by PC3 cells (Johnson et al., 2009). This observation further showed the important function of RBP for PC3 cells for riboflavin uptake.

A recent study showed the effect of Guinea pig serum riboflavin carrier protein (RCP) antisera on the HeLa cell line (human cervical cancer cell line) (Kudle et al., 2017). HeLa cancer cell lines showed IC50 values of 33.31 ± 0.7 for these antisera because of the depletion of riboflavin in cancer cell lines that led to cell growth inhibition since RBP could not carry riboflavin (Kudle et al., 2017).

Chapter 3

Materials and Methods

Isothermal Titration Calorimetry (ITC)

Materials

Riboflavin binding protein (10 μM) was prepared with phosphate buffer (pH 7.0, 50 x 10^{-3} M).The concentration of the riboflavin and lumichrome solutions, also prepared with phosphate buffer (pH 7.0, 50 x 10^{-3} M) was 100 μM whereas the concentration of the FMN and FAD was 500 μM.

Method

Binding of the four flavins to RBP was assessed by ITC (25 ^{o}C) using an AutoITC$_{200}$ (MicroCal, Inc., Northampton, MA). Prior to ITC, RBP was dialyzed overnight in phosphate buffer (pH, 7.0, 50 x 10^{-3} M). The protein (200 μL) was loaded into the reaction cell and 25, 1.5-μL aliquots of each flavin (ligand) were injected into the cell at 180-s intervals while the contents of the cell were stirred at a speed of 750-rpm. Data were analyzed using software Microanalysis, Origin Lab version 7.0 (OriginLabs, Inc., Northampton, MA) to calculate dissociation constants.

Fluorescence Spectroscopy

Materials

The protein, chicken egg white riboflavin binding protein (RBP), was obtained from Sigma- Aldrich (CAS # 91386-80-0). It was stored in the freezer, but, when it was prepared with phosphate buffer (Sigma–Aldrich, CAS #1805, diluted to 50 x 10^{-3} M), the solution was left at room temperature for several hours before experimentation. Four flavins were used for the research. They were also obtained from Sigma-Aldrich: riboflavin (CAS # 83-88-5), lumichrome (CAS# 3017990673), flavin mononucleotide (FMN) (CAS # F2253), and flavin adenine dinucleotide (FAD) (CAS # F6625). The flavins were stored in the freezer. Stock solutions of each flavin were prepared at a concentration of 1.0 x 10^{-3} M with phosphate buffer (pH 7.0, 50 x 10^{-3} M) and were stored in the refrigerator. Before the experiment was performed, the stock solutions were kept at room temperature for several hours. Because of riboflavin's sensitivity to light, it was always kept covered with aluminum foil.

Method

A Vernier Fluorescence/UV-VIS Spectrophotometer (VSP-FUV, Vernier.com) was used to assess the binding affinity of the flavin to RBP. For riboflavin and lumichrome, a Starna fluorescence quartz cuvette was used (Vernier.com, CUV-QUARTZ-FUV), and a rectangular sub-micro cuvette (Starna.com, 16.50-10/Z8.5) was used for the titration of FMN with RBP. LEDs of different wavelengths were provided with the spectrophotometer. The LED excitation wavelength for lumichrome was 375 nm and 450 nm for riboflavin and FMN. The parameters on

the spectrophotometer for each analysis were the following: sample time, 500; wavelength smoothing, 10; samples to average, 10; and LED intensity, 100. Various wavelength ranges were used for the flavins (Table 3.1). Three mL of the riboflavin and lumichrome stock solutions were prepared with phosphate buffer (pH 7.0, 50 x 10^{-3} M) and titrated with *u*L-aliquots of protein at an initial concentration of 1.35 x 10^{-3} M until the fluorescence of the flavin was quenched (Table 1); 0.25 mL was the initial volume of the FMN in the sub-micro cuvette. Because of the binding affinity of the different flavins to RBP, each flavin was quenched with a different total volume of RBP (Table 3.1).

A nonlinear regression, one site-specific binding, was used to obtain the binding affinity of the flavins using GraphPad Prism version 7.00 for Windows, GraphPad Software, La Jolla, California USA, www.graphpad.com. Logger Pro®, version 3.14.1, Vernier Software & Technology, Beaverton, Oregon was used to obtain the fluorescence data for the quenching of each flavin.

Table 3.1: The wavelength range, RBP aliquot, and total volume added to quench the flavins fluorescence

Flavin 4.4 x 10^{-4} M	**Wavelength Range (Å)**	**Riboflavin Binding Protein 1.35 x 10^{-3} M**	
		Aliquot (*u*L)	**Total volume (*u*L)**
Riboflavin	480–660	20.00	340
Lumichrome	420–590	20.00	260
FMN	480–700	10.00	120
FAD	Not completed		

Computational Chemistry

Methods: Choosing a Human Protein Structure Similar to Chicken RBP

Chicken RBP was used for the experimental research, but a human protein similar in structure to chicken RBP was used for the computational chemistry. The site, www.uniprot.org was used to search for chicken riboflavin binding protein and P02752 was found. BLAST resulted in alignment of P02752 with 4LRH.pdb, human folate receptor alpha. Human folate receptor alpha was used in conjunction with computational software, ICM-Pro (Molsoft, L.L.C.) to obtain the estimated binding energy (EBE) of the protein with each flavin. The flavins were docked a minimum of three times within an 8-Å radius of the potential binding site pocket. An average EBE was recorded. After docking and before computational assessment of the EBE, the best conformer provided by ICM-Pro was chosen based on using a combination of crystal structures from the Cambridge Structural Database. For the majority of molecules the first conformer provided by ICM-Pro was the one used to determine the EBE.

Chapter 4

Results

Isothermal Calorimetry Titration (ITC)

AutoITC200 (ITC) was used to collect the binding affinities of the four flavins (Figure 4.1) with riboflavin binding protein. The heat generated when the flavins were titrated into RBP was detected (Figures 4.2 and 4.3, top). The binding isotherms were created by plotting the integrated heat peaks against the molar ratio of flavins to RBP (Figures 4.2 and 4.3, bottom). The association constant (K) of each of the four flavins was measured by ITC (Figures 4.2 and 4.3). The binding affinity (dissociation constant) was calculated from the association constant using equation [4.1] (Kuriyan et al., 2009):

$$K_d = \frac{[P][L]}{[PL]} = \frac{1}{Ka} \qquad [4.1]$$

The binding energy (ΔG^0) was calculated from the binding affinity using equation [4.2] (Kuriyan *et al.*, 2009):

$$\Delta G^0_{bind} = RT \ln K_d \qquad [4.2]$$

The binding affinity and binding energy values for the flavins are summarized in Table 4.1.

Figure 4.1: The chemical structures of the four flavins

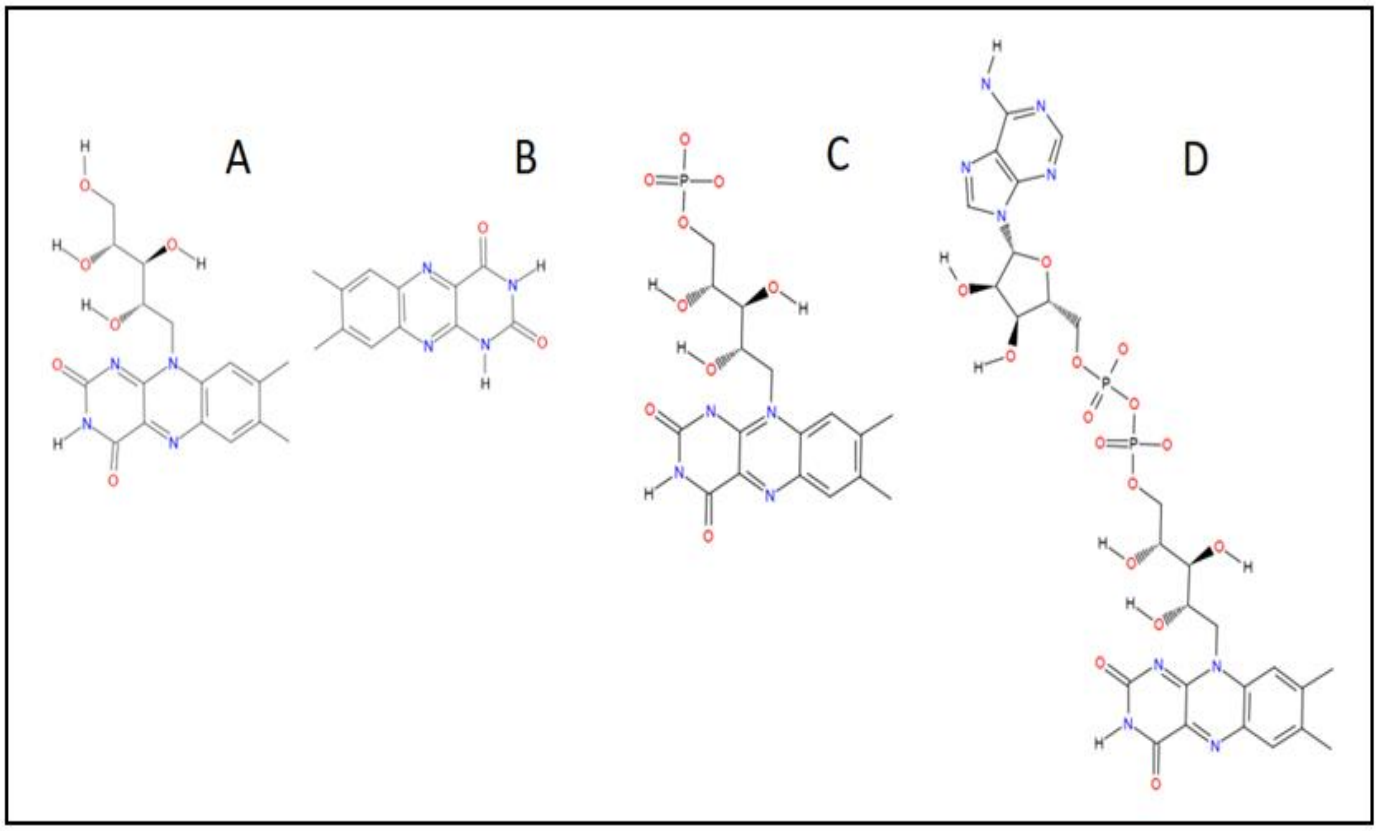

The chemical structures of the four flavins: riboflavin (**A**), lumichrome (**B**), FMN (**C**), and FAD (**D**). (ICM-Pro).

Figure 4.2: ITC determination of the binding thermodynamics of riboflavin and lumichrome to RBP

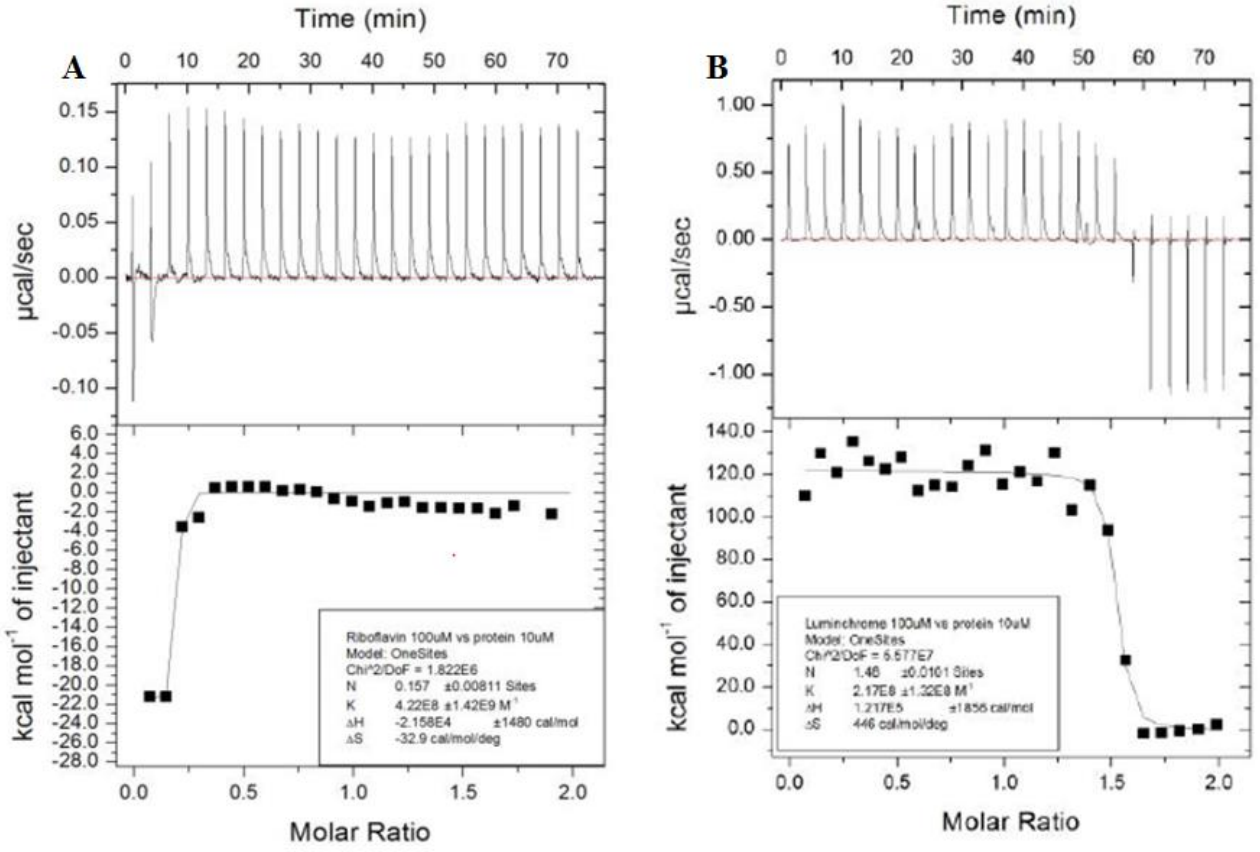

ITC determination of the binding thermodynamics of riboflavin and lumichrome to RBP. Titration of riboflavin (100 µM) into a solution of RBP (10 µM, **A**), and titration of lumichrome (100 µM) into a solution of RBP (10 µM, **B**). The experiments were performed in 50 x 10^{-3} M phosphate buffer, pH 7.0 at 25°C. The injection volume is 1.5 µl and 25 injections were used. Analysis of the two sets of data yields the association constant of riboflavin and lumichrome.

Figure 4.3: ITC determination of the binding thermodynamics of FMN and FAD to RBP

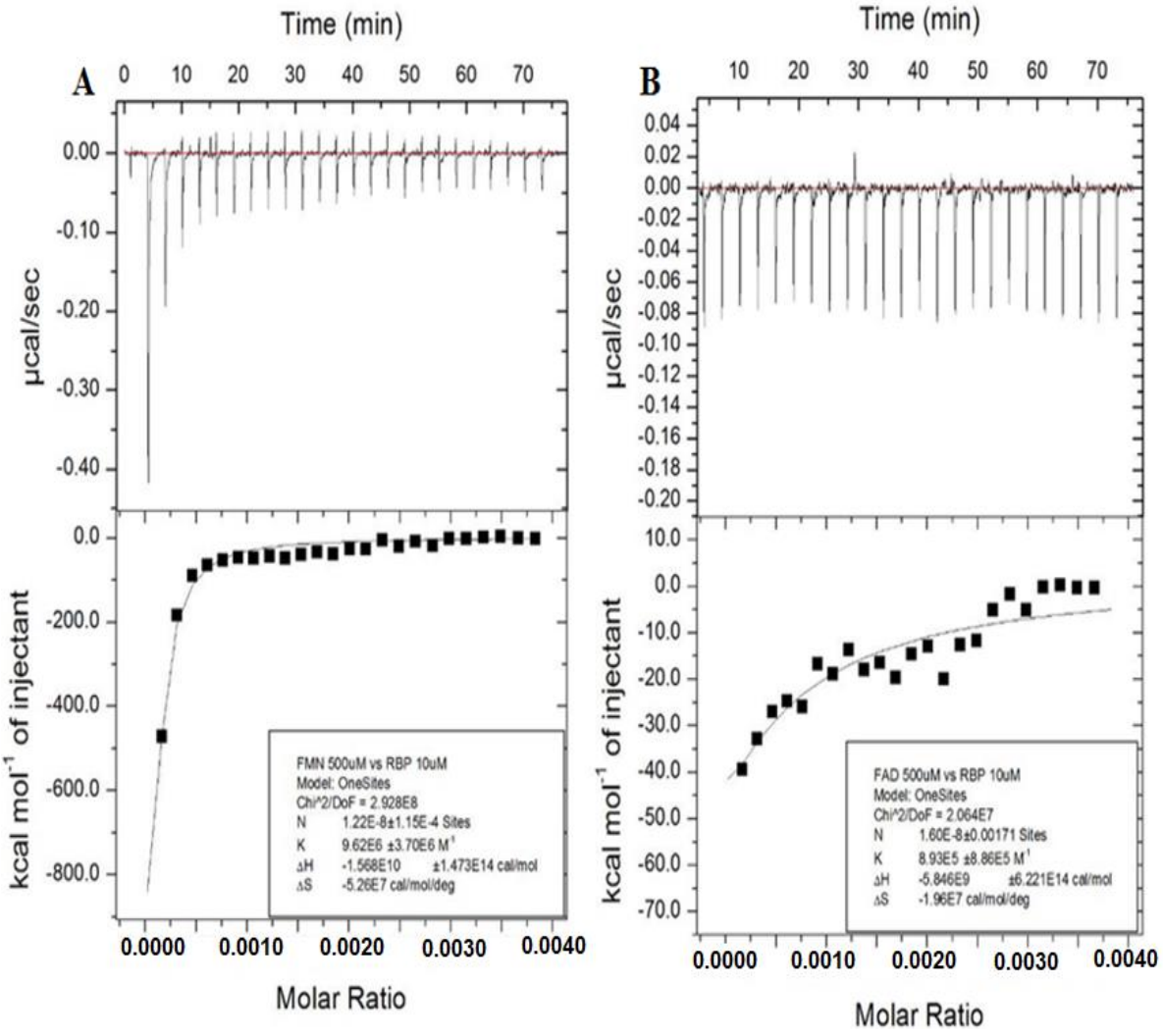

ITC determination of the binding thermodynamics of FMN and FAD to RBP. Titration of FMN (500 µM) into a solution of RBP (10 µM, **A**), and titration of FAD (500 µM) into a solution of RBP (10 µM, **B**). The experiments were performed in 50 x 10^{-3} M phosphate buffer, pH 7.0 at 25°C. The injection volume is 1.5 µl and 25 injections were used. Analysis of the two sets of data yields the association constant of FAD and FMN.

Table 4.1: The measured binding affinity (K_d) and binding energy (ΔG^0) of the four flavins to RBP using ITC

Flavin	Dissociation constant (Binding Energy) (K_d) (M)	Calculated Binding Energy (ΔG^0) (kcal/mole)
FAD	1.116×10^{-6}	- 8.115
FMN	1.039×10^{-7}	- 9.521
Lumichrome	4.600×10^{-9}	- 11.36
Riboflavin	2.360×10^{-9}	- 11.76

Fluorescence Spectrometry

A Vernier Fluorescence/UV-VIS Spectrophotometer was used to measure binding affinity values for the three flavins (Table 4.2). Titration of the flavins with RBP was monitored by fluorescence spectrometry and is shown in Figure 4.4. The data from Figure 4 were analyzed using equation [4.3] (Motulsky, 2018). A plot of ($\frac{\Delta F}{\Delta Fmax} = \alpha = \frac{[RBP]}{Kd+[RBP]}$) (Chenprakhon, 2010**)** versus the concentration of free RBP was used to calculate K_d for the flavins (Figure 4.5).

$Y = Bmax*X/(K_d + X)$ [4.3]

Figure 4.4: The quenching of flavin fluorescence RBP

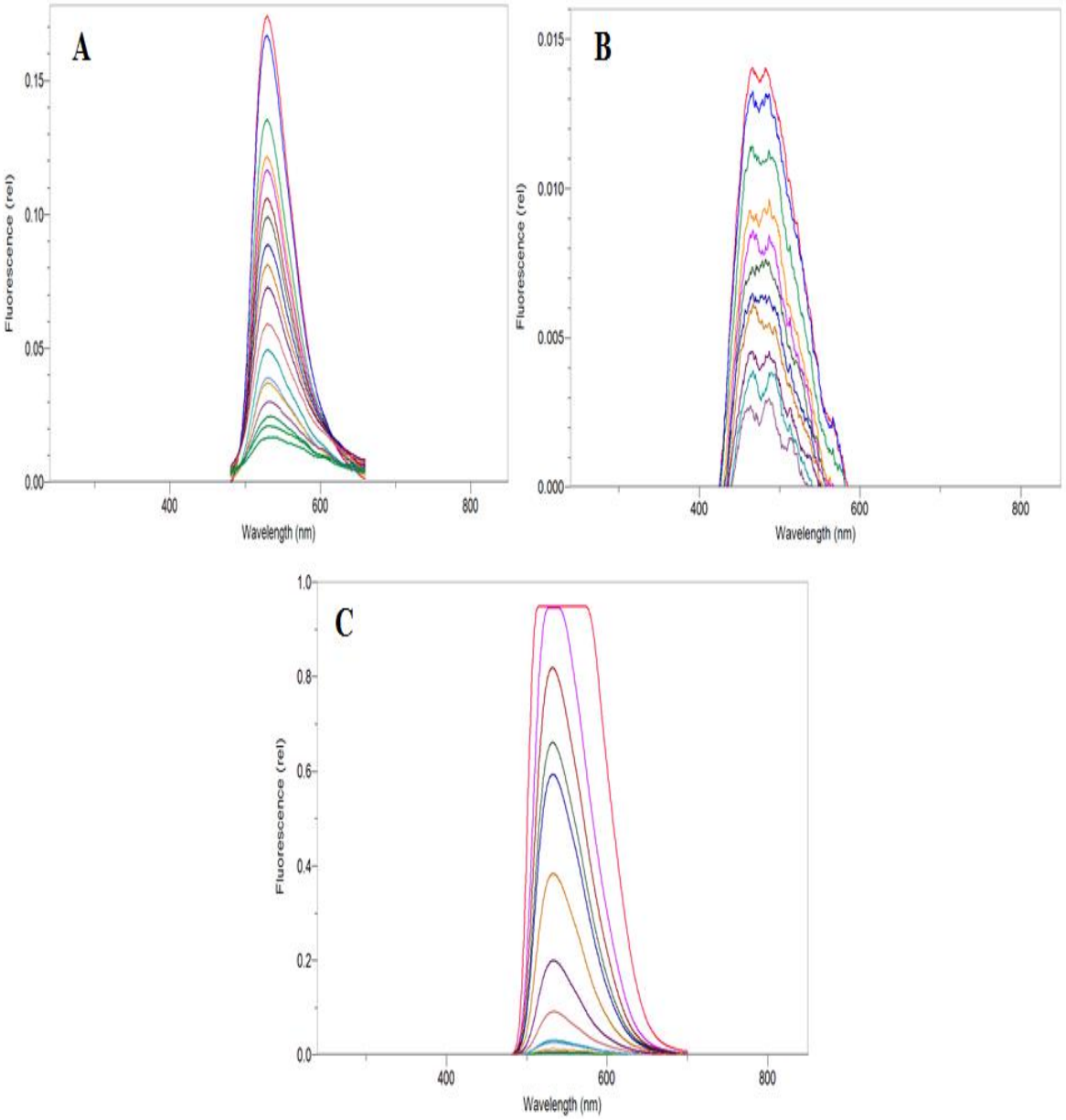

The quenching of flavin fluorescence RBP. Titration of RBP (1.35 x 10^{-3} mol L^{-1}) into a solution of flavin (4.4 x10^{-4} mol L^{-1}; **A**), lumichrome (4.4 x10^{-4} mol L^{-1}; **B**), and FMN (4.4 x10^{-4} mol L^{-1}; **C**). The experiments were performed in 50 x 10^{-3} M phosphate buffer, pH 7.0 at 25°C. Analysis of these graphs yields the dissociation constant for each of the three flavins (Figure 4.5).

Figure 4.5: Plots of the flavins quenched fluorescence from Figure 4.4

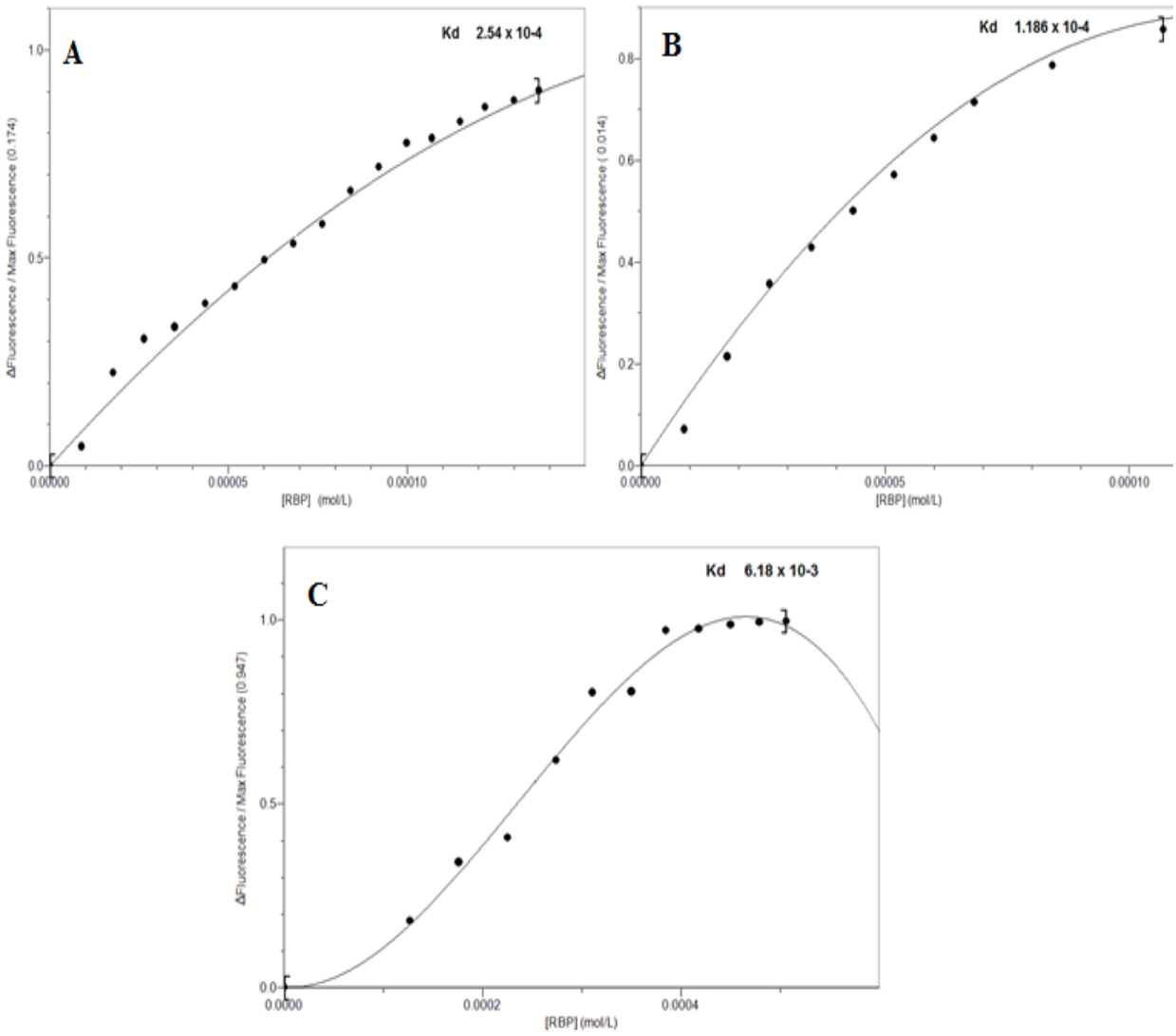

Plots of the flavins' quenched fluorescence from Figure 4.4. The data of the fluorescence quenching for each of the flavins reported in Figure 4.4 are analyzed according to [Y = Bmax*X/(K_d + X)] using nonlinear regression analysis, one site-specific binding (Motulsky, 2018). ($\frac{\Delta F}{\Delta Fmax} = \alpha = \frac{[RBP]}{Kd+[RBP]}$) (Chenprakhon, 2010) was plotted versus the concentration of free RBP to calculate the K_d values for riboflavin (**A**), lumichrome (**B**), and FMN (**C**)

Table 4.2: The measured binding affinities (K_d) and calculated binding energy (ΔG^0) for the flavins in RBP using fluorescence spectrometry

Flavin	Dissociation constant Binding Affinity (K_d) (M)	Calculated Binding Energy (ΔG^0) (kcal/mole)
FAD	N/A	N/A
FMN	6.230×10^{-3}	-3.011
Lumichrome	1.186×10^{-4}	-5.360
Riboflavin	2.540×10^{-4}	-4.908

ICM-Pro

The values of estimated binding energy (ΔG^0) from ICM-Pro and calculated binding affinity are summarized in Table 3. The FAD had the most negative ΔG^0 value (-21.43 kcal/mole) and the smallest K_d value (2.020×10^{-16} M).

ICM-Pro (Abagyan et al., 1994) was used to identify the four flavins as drug-like or nondrug-like molecules (Figures 4.6 and 4.7). The riboflavin and lumichrome were categorized as drug-like molecules because they satisfied Lipinski's "Rule of Five" (Figure 4.6). The "Rule of Five" is used for predicting oral bioavailability and has the following parameters: no more than 5 hydrogen bond donors (HBD); no more than 10 hydrogen bond acceptors (HBA); molecular mass less than 500 daltons; and Log *P* not greater than 5 (Lipinski, 2004).
FMN had an unacceptable number of hydrogen bond donors (HBD), and hydrogen bond acceptors (HBA), and FAD had unacceptable values for all of Lipinski's "Rule of Five" parameters. Thus, FAD and FMN were categorized as nondrug-like molecules (Figure 4.7).

Table 4.3: The ICM-Pro estimated binding energy (ΔG^0) and calculated binding affinity (K_d) of the flavins using 4LRH.pdb

Flavin	Estimated Binding Energy (ΔG^0) (kcal/mole)	Calculated Binding Affinity (K_d) (M)
FAD	- 21.43	2.020×10^{-16}
FMN	- 14.57	2.135×10^{-11}
Lumichrome	- 3.300	3.383×10^{-3}
Riboflavin	- 6.696	1.248×10^{-5}

Figure 4.6: Drug-like molecules, riboflavin and lumichrome, and their molecular weight, number of HBA, number of HBD, and MolLog P value

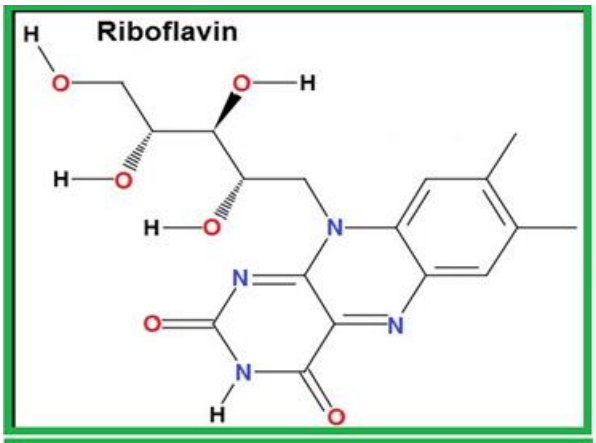

MolWeight	376.1383
HBA	10
HBD	5
MolLogP	-1.75117

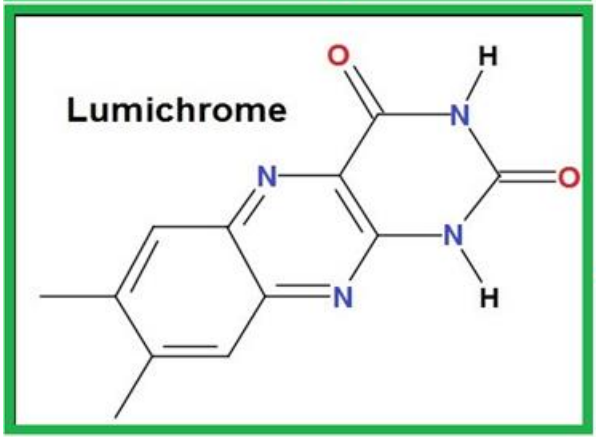

MolWeight	242.0804
HBA	6
HBD	2
MolLogP	1.4626

Figure 4.7: Non-drug like molecules, FAD and FMN, and their molecular weight, number of HBA, number of HBD, and MolLog P value

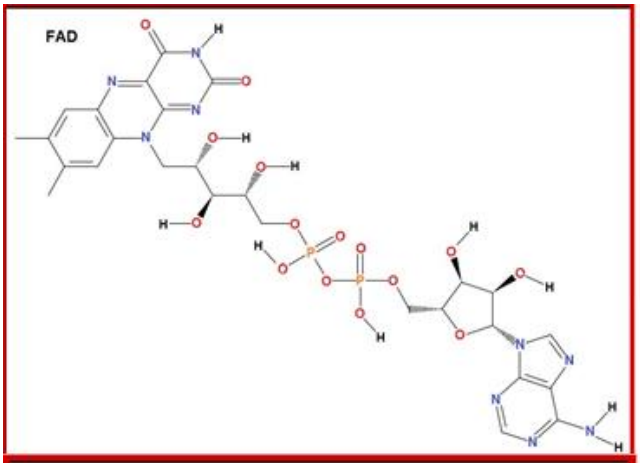

MolWeight	785.1571
HBA	24
HBD	10
MolLogP	-6.55113

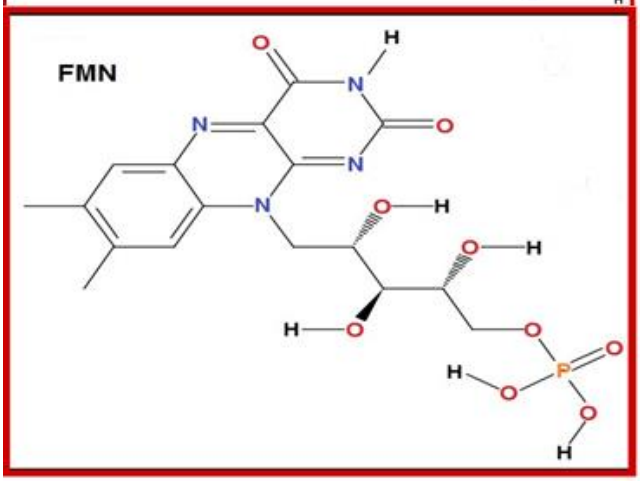

MolWeight	456.1046
HBA	14
HBD	6
MolLogP	-3.45149

Comparison of the Binding Energy (ΔG^0)

To compare the binding energy of the flavins, ICM-Pro was used to computationally calculate ΔG^0 and the K_d value from ITC, and fluorescence spectrometry was used to calculate the binding energy (Figure 4.8). The binding energy of FAD from fluorescence spectrometry is not included because it was not determined. When the binding energy of FMN, lumichrome and riboflavin are compared, ITC showed more negative values compared with fluorescence spectrometry (Figure 4.8). The average difference between the ITC and fluorescence spectrometry binding energy values for the three flavins is approximately 6.5 kcal/mole (Table 4.4). Despite the discrepancy of ITC and fluorescence spectrometry binding energy values, there is an approximate consistent difference between their values (Table 4.4).

The binding energy values from ICM-Pro are more negative than the ITC values for FAD and FMN, whereas the lumichrome and riboflavin values from ICM-Pro are less negative than the ones from ITC (Figure 4.8). The approximate difference between the ITC and ICM-Pro binding energy values for each of the FMN and Riboflavin is approximately 5 kcal/mole, but for lumichrome and FAD the approximate difference is 8 and 13 kcal/mole, respectively (Table 4.5).

Comparison of the Binding Affinity (K_d)

The binding affinity values of the flavins are shown in Figure 4.9. The binding affinity value for each of the four flavins was obtained experimentally using fluorescence spectroscopy and ITC and was calculated from the computational estimated binding energy (ΔG^0) value from ICM-Pro.

The binding affinity (K_d) values of the flavins were compared just like the binding energy values were. The binding affinity of FAD from fluorescence spectrometry is not included because it was not determined. ITC showed smaller K_d values for FMN, lumichrome, and riboflavin when compared with fluorescence spectrometry (Figure 4.9). The average difference between the ITC and fluorescence spectrometry binding affinity values for the three flavins is approximately 4.735 (Table 4.4). Despite the discrepancy of ITC and fluorescence spectrometry binding affinity values, there is an approximate consistent difference between their values (Table 4.4).

The binding affinity values from ICM-Pro are smaller than the ITC values for FAD and FMN, whereas the lumichrome and riboflavin values from ICM-pro are smaller than the ones from ITC (Figure 4.9). The average difference between the ITC and ICM-Pro binding affinity values for each of the FMN and riboflavin is approximately 3.705, but for lumichrome and FAD the approximate difference is 5.920 and 9.742, respectively (Table 4.5).

Figure 4.8: The binding energies for FMN, FAD, lumichrome, and riboflavin using ITC, ICM-Pro, and fluorescence spectrometry

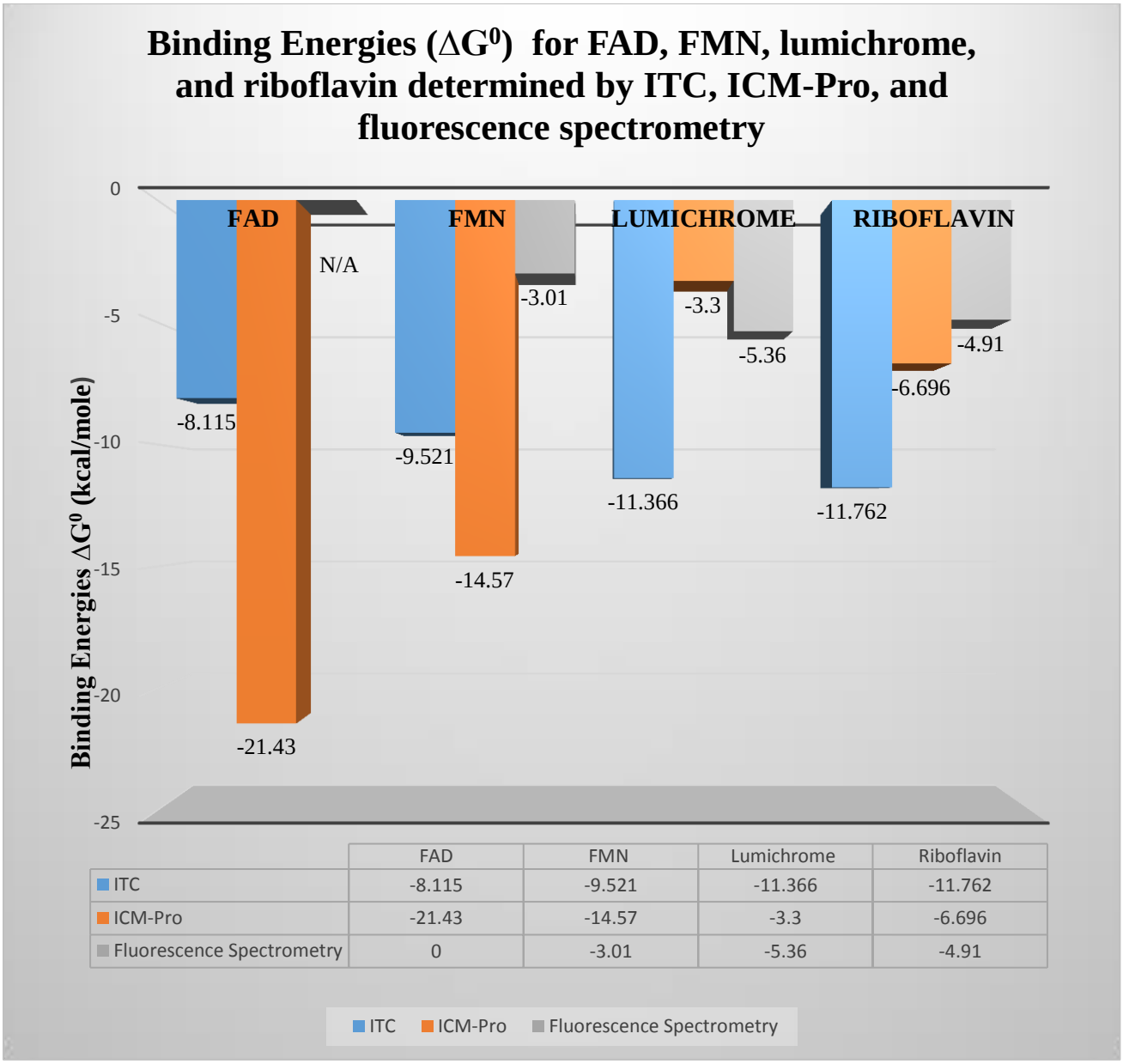

Table 4.4: The difference between ITC and fluorescence spectrometry K_d and ΔG^0 for FMN, lumichrome, and riboflavin

	Differences between ITC and fluorescence spectrometry values	
Flavin	K_d	ΔG^0
FMN	4.778	6.511
Lumichrome	4.411	6.006
Riboflavin	5.016	6.852

Figure 4.9: Binding affinities (K_d) for FAD, FMN, lumichrome, and riboflavin determined by ITC, ICM-Pro, and fluorescence spectrometry

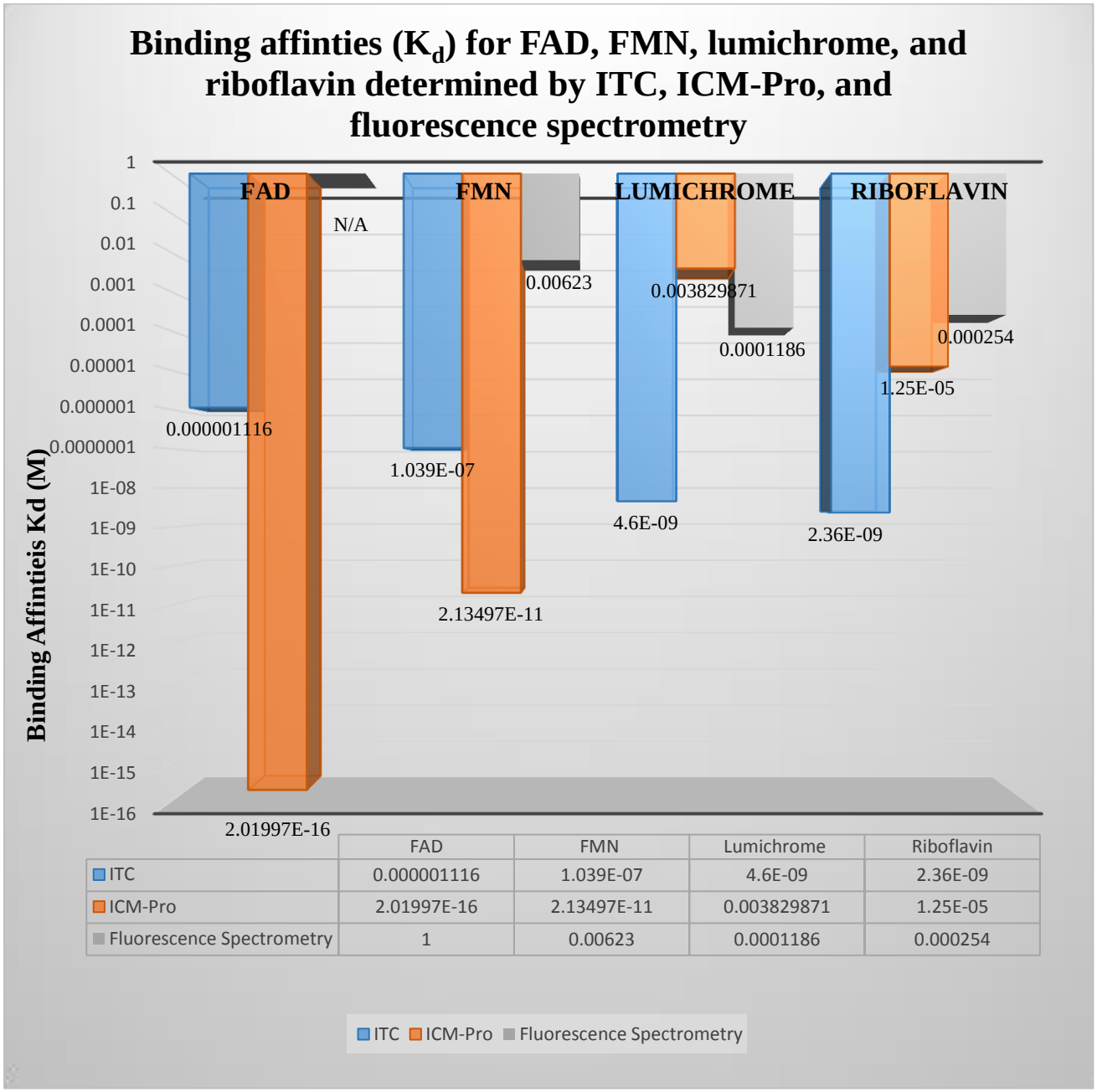

	FAD	FMN	Lumichrome	Riboflavin
ITC	0.000001116	1.039E-07	4.6E-09	2.36E-09
ICM-Pro	2.01997E-16	2.13497E-11	0.003829871	1.25E-05
Fluorescence Spectrometry	1	0.00623	0.0001186	0.000254

Table 4.5: The difference between ITC and ICM-Pro K_d and ΔG^0 values for FAD, FMN, lumichrome, and riboflavin

	Differences between ITC and ICM-Pro values	
Flavin	K_d	ΔG^0
FAD	9.742	13.315
FMN	3.687	5.049
Lumichrome	5.920	8.066
Riboflavin	3.7239	5.066

Sequence and Structural Comparison

Basic Local Alignment Search Tool (BLAST) was used to find the closest homologous protein to riboflavin binding protein (Figure 4.10). Human folate receptor alpha, 4LRH.pdb was found to be the closest in sequence similarity to RBP (identity 33%, positive 48 %).

Five areas were chosen to be highlighted using UniProt as shown in Figures 4.11 and 4.12. Identical and similar amino acids between both proteins are shown in Figure 4.11A as dark grey and light grey, respectively. Figure 4.11B shows the conserved cysteine amino acids. In Figure 4.12 hydrophobic amino acids (A), polar amino acids (B), and aromatic amino acids (C) are highlighted.

Figure 4.10: Amino acid sequence alignment of RBP and 4LRH.pdb using BLAST

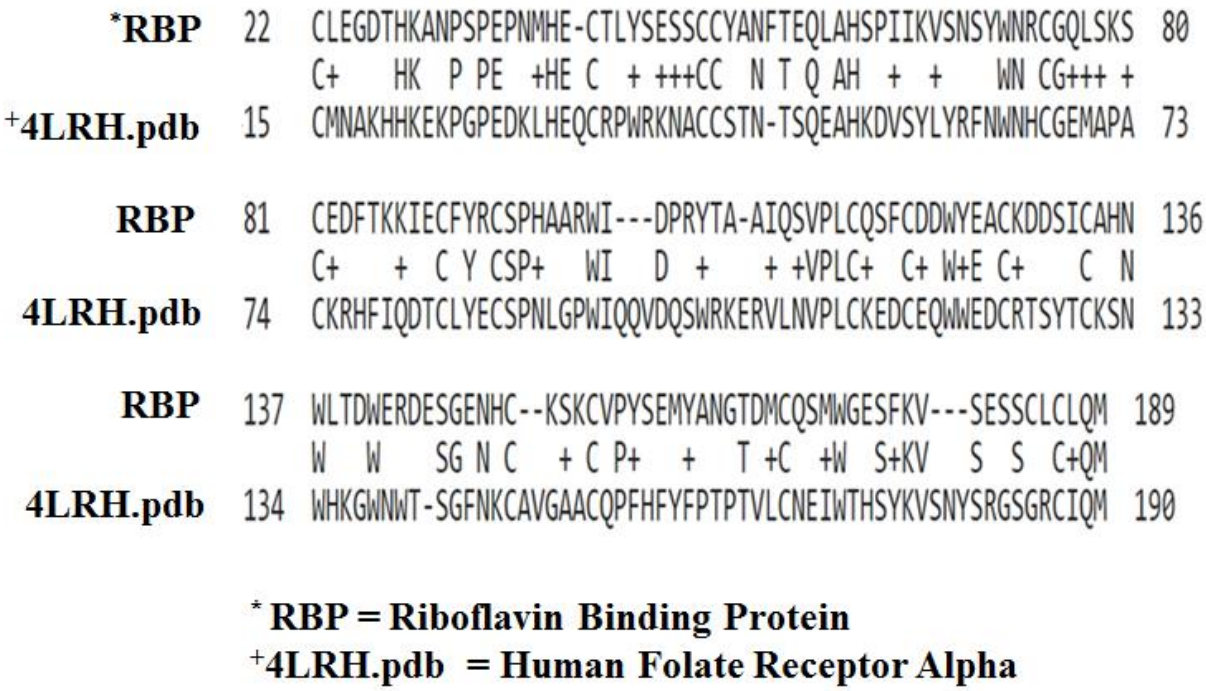

Amino acid sequence alignment of RBP and 4LRH.pdb using BLAST. Identical amino acids are shown between RBP and 4LRH.pdb. Positives refer to similar but not identical amino acids. The expectation value (E-value) for this alignment was 10^{-23}.

Figure 4.11: Amino acid sequence alignment of RBP and 4LRH.pdb using UniProt

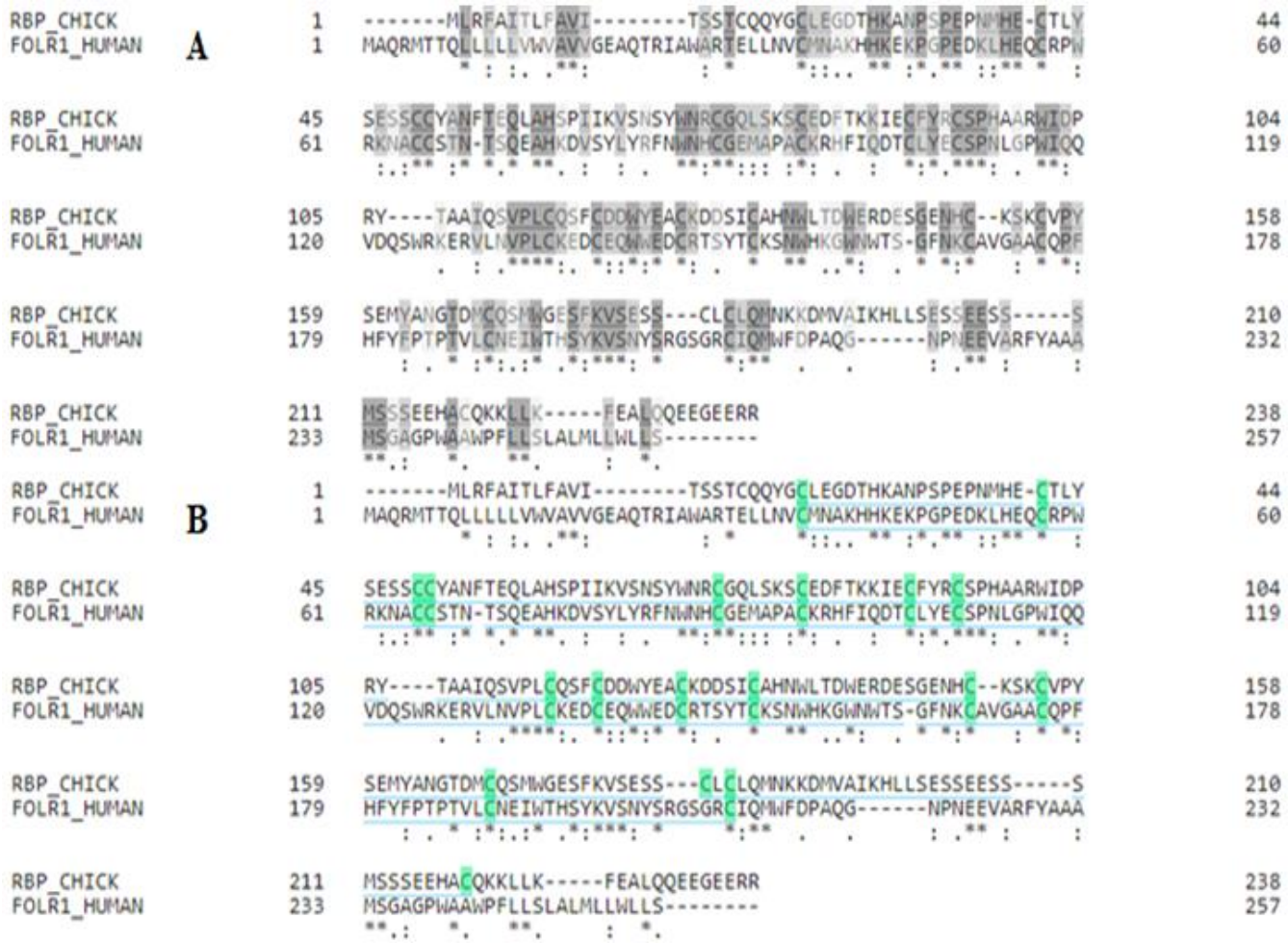

Amino acid sequence alignment of RBP and 4LRH.pdb using UniProt. Identical and similar amino acids are highlighted in dark grey and light grey, respectively (**A**). Disulfide bonds are highlighted in green (**B**).

Figure 4.12: Amino acid sequence alignment of RBP and 4LRH.pdb using UniProt

Amino acid sequence alignment of RBP and 4LRH.pdb using UniProt. Hydrophobic amino acids are highlighted in blue (**A**), polar amino acids in purple (**B**), and aromatic amino acids in pink (**C**).

Each of the four flavins was docked into the active site of human folate receptor alpha (4LRH.pdb) using ICM-Pro (Molsoft, L.L.C) (Figure 4.13). In addition, their estimated binding energies were computationally determined and the binding affinities were calculated (Table 4.3). Amino acids that were near the active site within an 8 Å radius of the active site pocket are highlighted in Figure 4.14.

The position of riboflavin in the crystalized RBP binding site (Monaco, 1997) (Figure 4.15) was compared to the position of riboflavin in the 4LRH.pdb binding site in ICM-Pro (Figure 4.16). The riboflavin was found to have a similar position in 4LRH.pdb and the RBP binding site (Figures 4.15 and 4.16). RBP amino acids were numbered by Monaco (1997) and their corresponding amino acids in 4LRH.pdb were numbered according to ICM-Pro. The xylene moiety of the riboflavin isoalloxazine moiety was stacked in between the rings of Tyr75 and Trp156 of RBP (Figure 4.15) (Monaco, 1997). In 4LRH.pdb, the riboflavin was also stacked in between the rings of the Tyr85 and Trp156, which are the corresponding amino acids of Tyr75 and Trp156, respectively, from RBP (Figure 4.16). Tyr 75 and Trp156 from RBP and their corresponding amino acids from 4LRH.pdb Tyr85 and Trp171, respectively, are highlighted in yellow (Figure 4.17).

Figure 4.13: The flavins docked into the active site of 4LRH.pdb

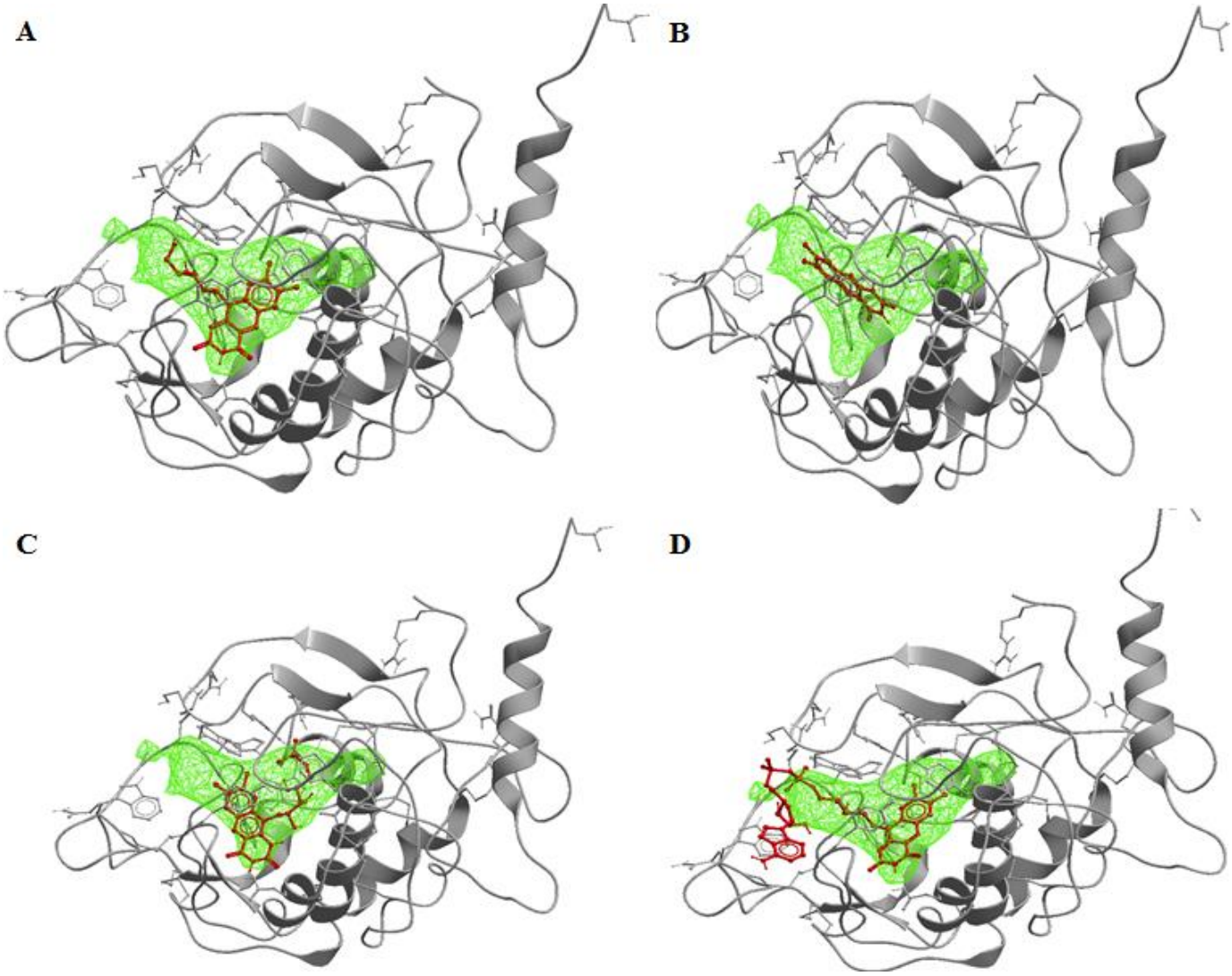

The flavins docked into the active site of 4LRH.pdb. The protein is colored with grey, flavins with red and the binding pocket with green. The four flavins were docked into the protein using ICM-Pro (Molsoft, L.L.C), riboflavin (**A**), lumichrome (**B**), FMN (**C**), and FAD (**D**).

Figure 4.14: 4LRH.pdb binding site amino acids

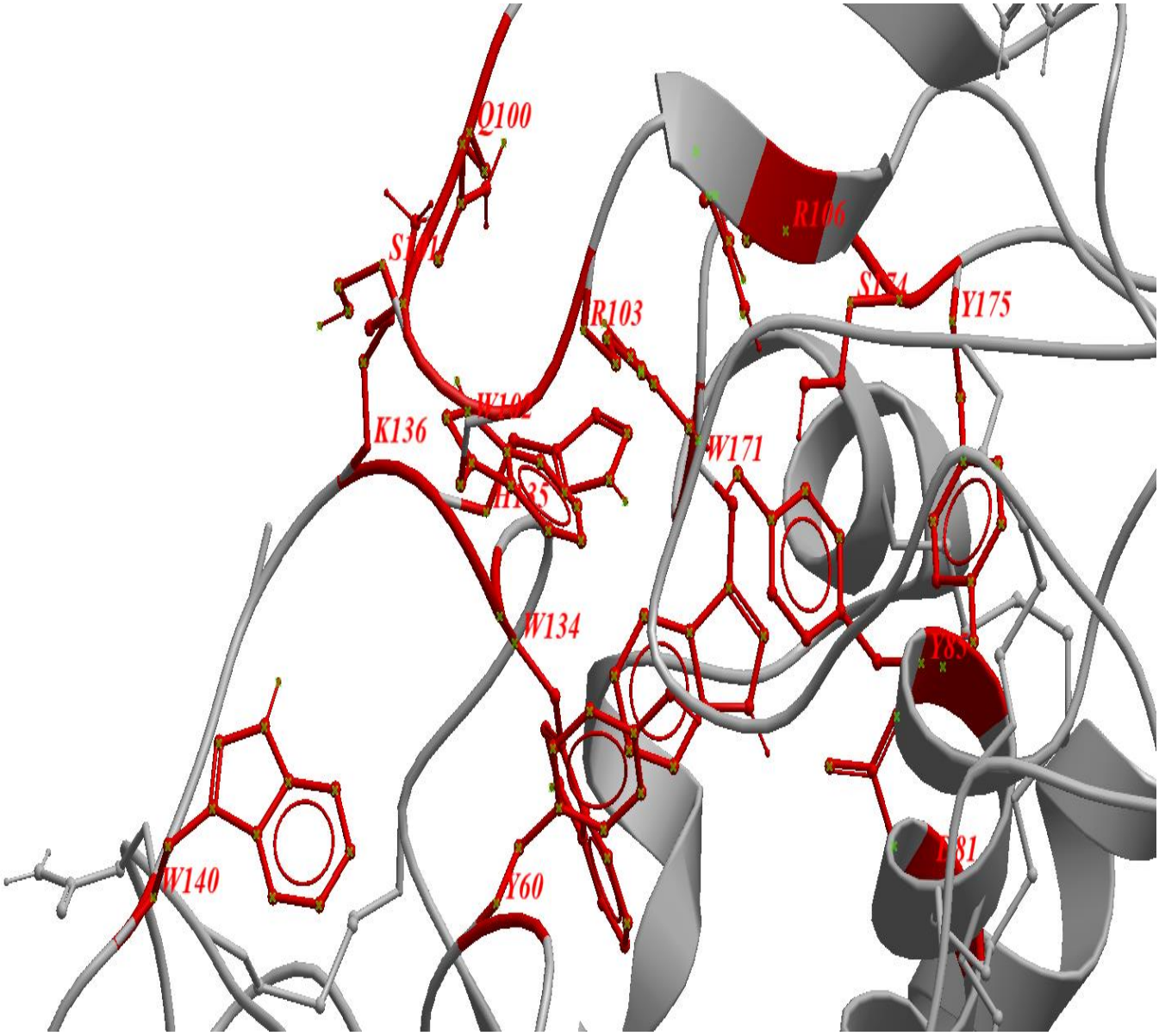

4LRH.pdb binding site amino acids. The active site amino acids are colored with red and the protein with grey.

Figure 4.15: The position of riboflavin in the active site of the crystalized RBP

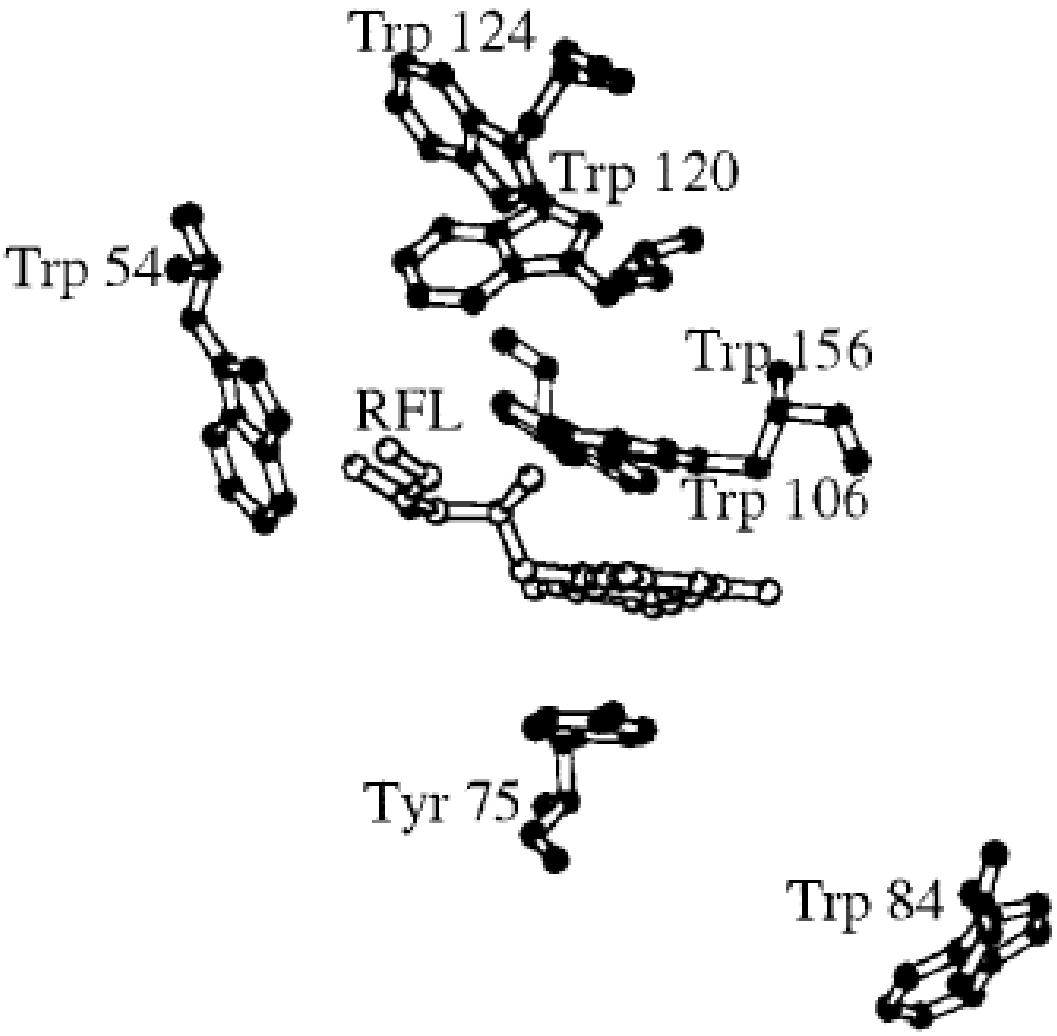

The position of riboflavin in the active site of the crystalized RBP. (Monaco, 1997).

Figure 4.16: The position of riboflavin molecule with respect to Tyr85 and Trp171 in the 4LRH.pdb binding site in ICM-Pro

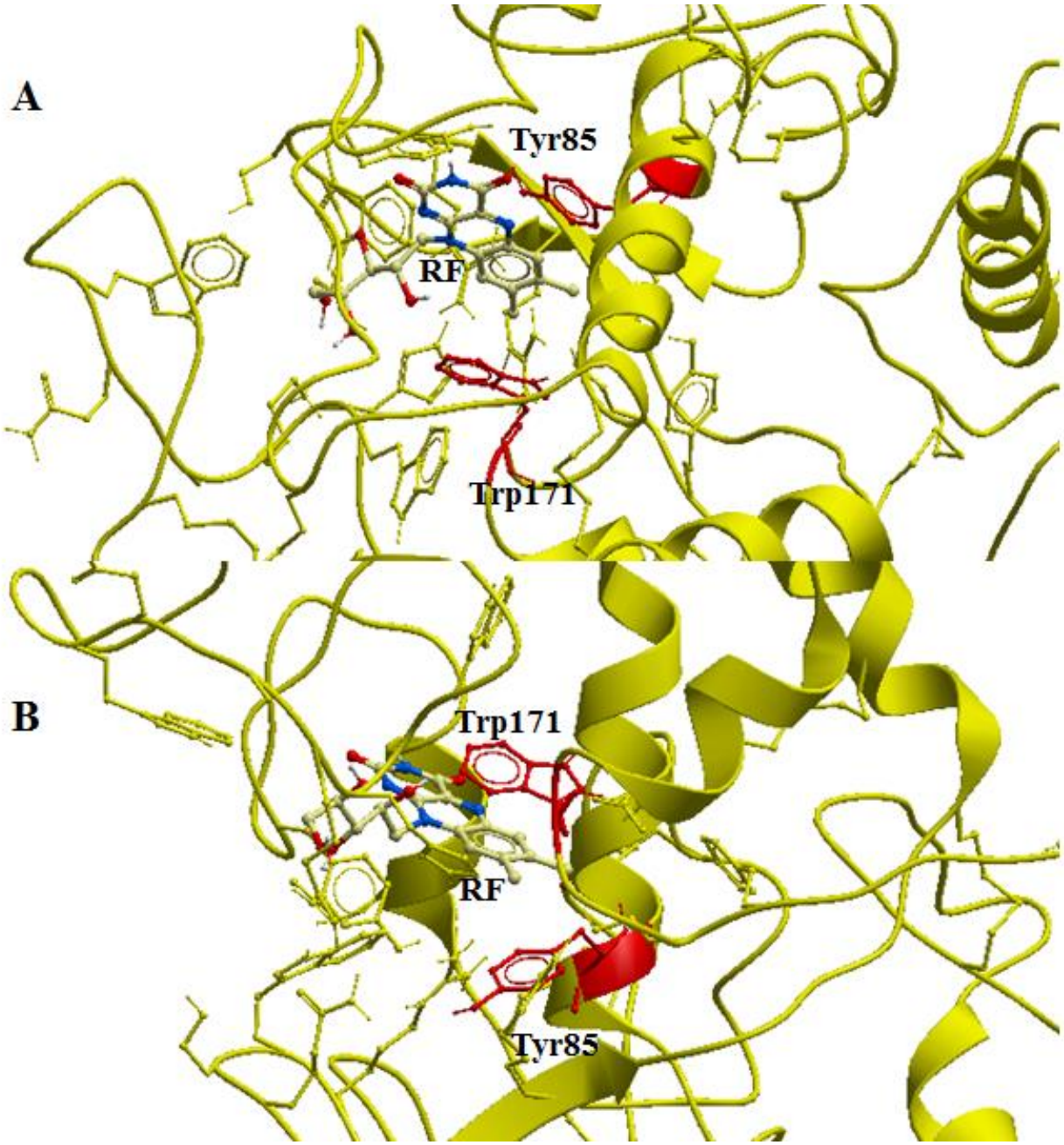

Figure 4.17: Aligned amino acid sequences of RBP and 4LRH.pdb using UniProt

```
RBP_CHICK   SESSCCYANFTEQLAHSPIIKVSNSYWNRCGQLSKSCEDFTKKIECFYRCSPHAARWIDP 104
FOLR1_HUMAN RKNACCSTN-TSQEAHKDVSYLYRFNWNHCGEMAPACKRHFIQDTCLYECSPNLGPWIQQ 119

RBP_CHICK   RY----TAAIQSVPLCQSFCDDWYEACKDDSICAHNWLTDWERDESGENHC--KSKCVPY 158
FOLR1_HUMAN VDQSWRKERVLNVPLCKEDCEQWWEDCRTSYTCKSNWHKGWNWTS-GFNKCAVGAACQPF 178

RBP_CHICK   SEMYANGTDMCQSMWGESFKVSESS---CLCLQMNKKDMVAIKHLLSESSEESS-----S 210
FOLR1_HUMAN HFYFPTPTVLCNEIWTHSYKVSNYSRGSGRCIQMWFDPAQG------NPNEEVARFYAAA 232

RBP_CHICK   MSSSEEHACQKKLLK-----FEALQQEEGEERR 238
FOLR1_HUMAN MSGAGPWAAWPFLLSLALMLLWLLS-------- 257
```

Aligned amino acid sequences of RBP and 4LRH.pdb using UniProt. Tyr75 and Trp156 from RBP and their corresponding amino acids in 4LRH.pdb are highlighted in yellow. The four Tryptophan amino acids (Trp 54, 106, 120, and 124) from RBP and their corresponding amino acids in 4LRH.pdb are highlighted in green. Amino acids that form hydrogen bonds with riboflavin in 4LRH.pdb are highlighted in light blue.

The distance of Tyr85 and Trp171 from the riboflavin in 4LRH.pdb binding site was measured using ICM-Pro (Molsoft, L.L.C) (Figure 4.18). The distance of the Tyr85 plane and riboflavin (RF) xylene moiety plane was measured as 4.31 Å (Figure 4.18A). The Trp171 plane was measured as 4.0 Å from the riboflavin xylene moiety plane (Figure 4.18B). In the crystallized RBP binding site the Tyr75 plane was 3.7 Å from the riboflavin xylene moiety plane and the Trp156 plane was 3.7 Å from the riboflavin xylene moiety plane (Monaco, 1997). Four tryptophan amino acids (Trp 54, 106, 120, and 124) were reported to be in the vicinity of the riboflavin molecule in the RBP active site (Monaco, 1997). In 4LRH.pdb, Trp64, which is the corresponding amino acid of Trp54 from RBP, was measured to be closer to riboflavin (4.13

Å) than the other three tryptophan amino acids (Trp 120, 134, and 138) (Figure 4.19A). The distance between each of Trp 120, 134, and 138, that are the corresponding amino acids of Trp 106, 120, and 124, respectively from RBP, and riboflavin was measured (Figure 4.19B). These four tryptophan amino acids are highlighted in green (Figure 4.17).

Four amino acids were found to have hydrogen bonds with the riboflavin molecule in the active site of 4LRH.pdb. The distances of the hydrogen bonds between the four amino acids (Ser57, Phe62, Trp134, and His138) and riboflavin were measured using ICM-Pro (Figure 4.20 A and B). These amino acids are highlighted in light blue (Figure 4.17).

Ligand 2-D interaction models were created for the four flavins in the 4LRH.pdb binding site as shown in ICM-Pro (Figure 4.21). These models show the hydrophobic interactions and hydrogen bonds between the four flavins and the 4LRH.pdb binding site amino acids.

Figure 4.18: The distance of Tyr 85 and Trp171 from the riboflavin molecule (RF) in the 4LRH.pdb binding site in ICM-Pro

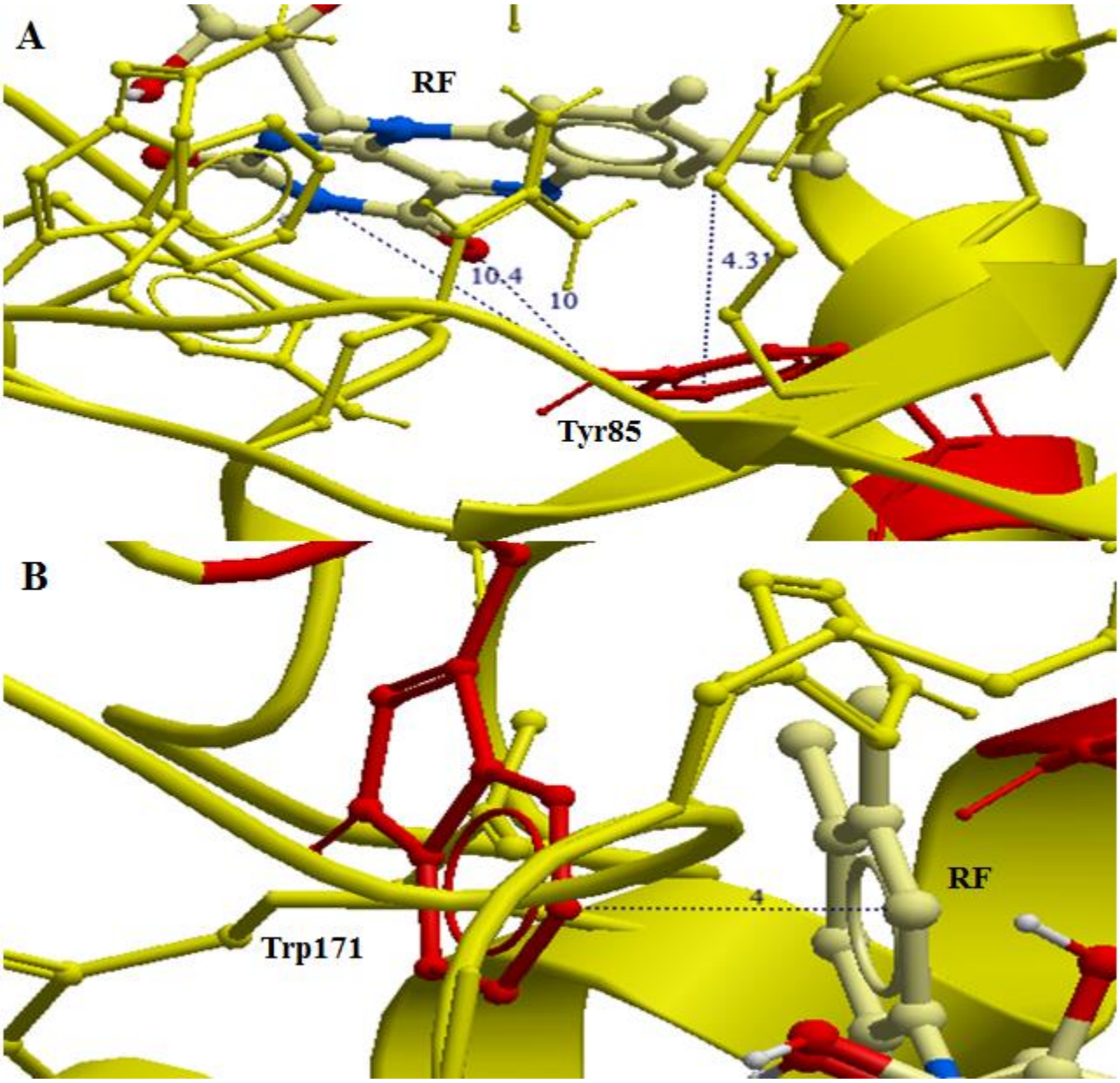

The distance of Tyr85 and Trp171 from the riboflavin molecule (RF) in the 4LRH.pdb binding site in ICM-Pro. The distance of Tyr85 from riboflavin **(A)**, and the distance of Trp171 from riboflavin (**B)** was measured using ICM-Pro.

Figure 4.19: The distance of Trp64, Trp120, Trp134 and Trp138 from riboflavin (RF) in the 4LRH.pdb binding site in ICM-Pro

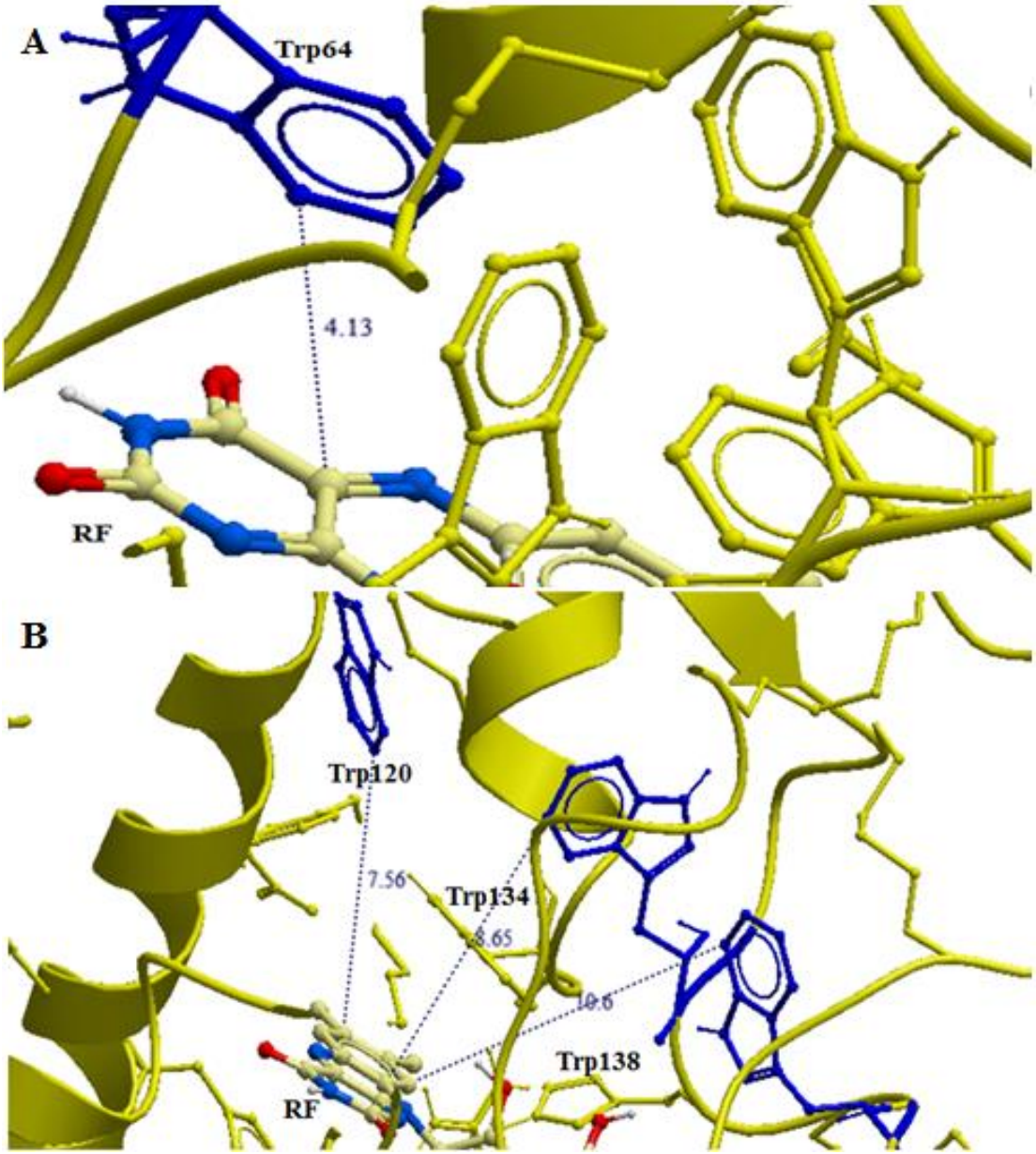

The distance of Trp64, Trp120, Trp134, and Trp138 from riboflavin (RF) in the 4LRH.pdb binding site in ICM-Pro. The distance of Trp64 from riboflavin **(A)**, and of (Trp120, Trp134, and Trp138) from riboflavin **(B)** was measured using ICM-Pro.

Figure 4.20: The measurements of the four hydrogen bonds with riboflavin (RF) in the 4LRH.pdb binding site in ICM-Pro

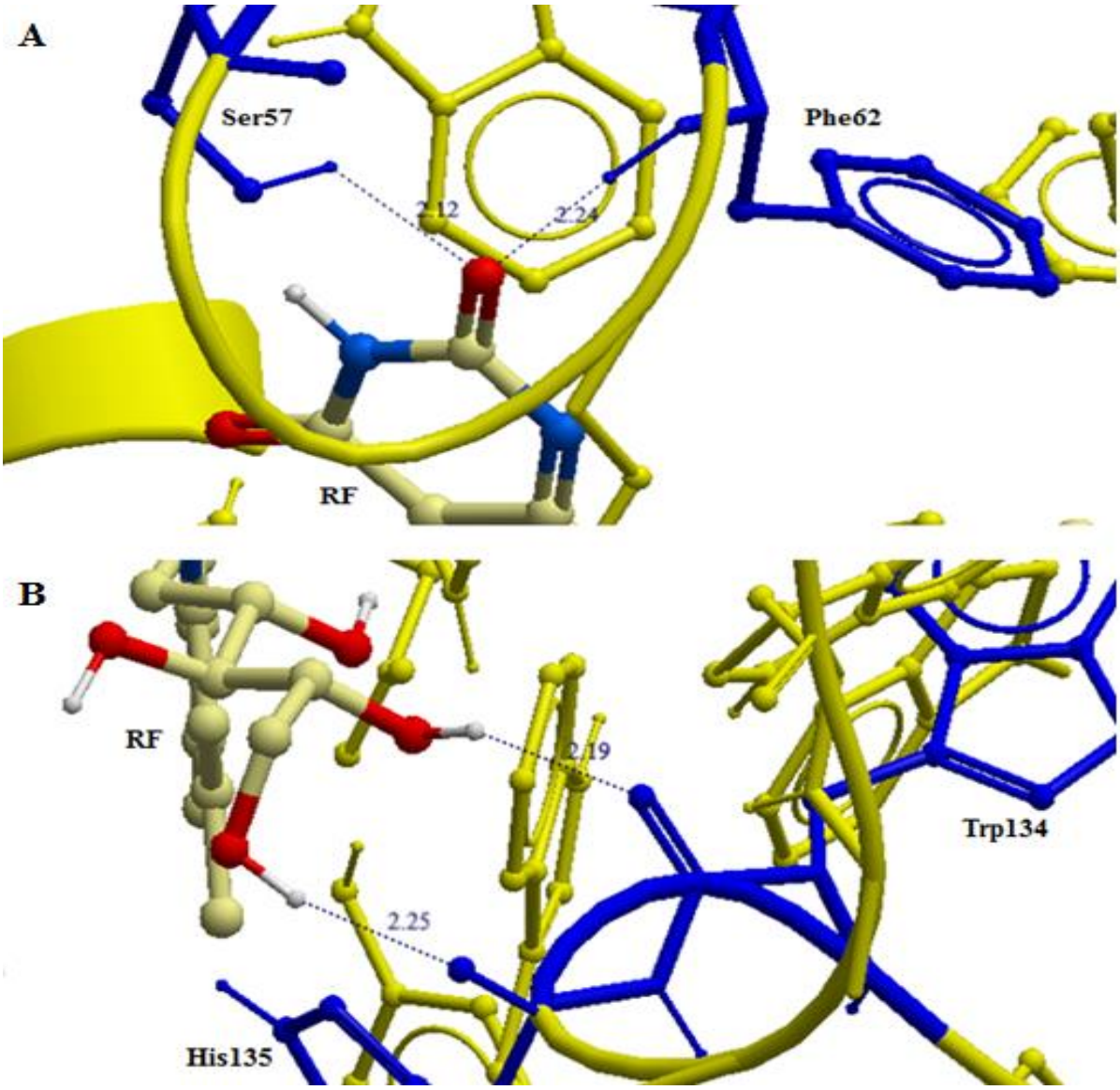

The measurements of the four hydrogen bonds with riboflavin in 4LRH.pdb binding site in ICM-Pro. A shows the two hydrogen bonds formed between Ser57 and riboflavin (RF) and between Phe62 and RF. **B** shows the two hydrogen bonds formed between Trp134 and riboflavin (RF) and between His138 and RF. These hydrogen bonds were measured using ICM-Pro.

Figure 4.21: Ligand 2-D interaction model for the four flavins in the 4LRH.pdb binding site in ICM-Pro

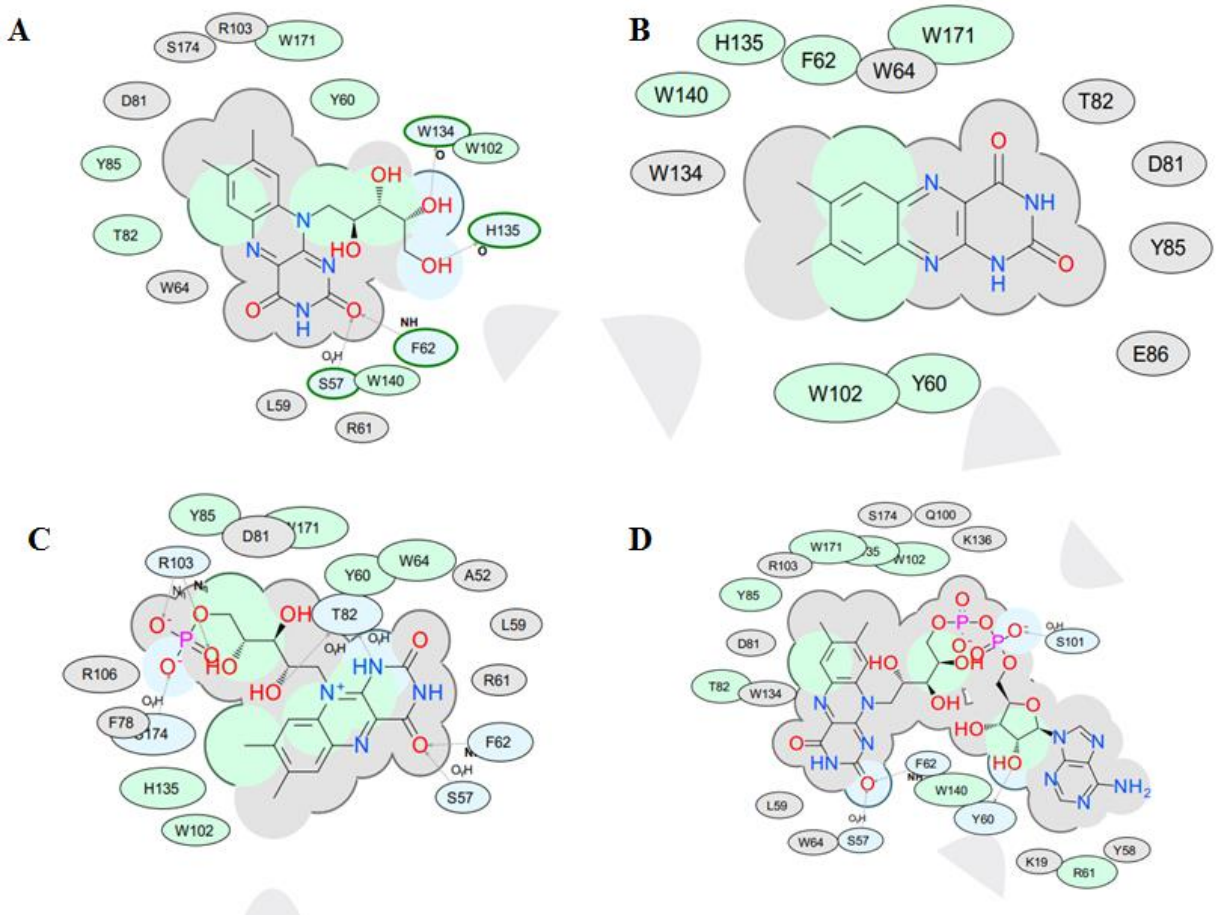

Ligand 2-D interaction model for the four flavins in the 4LRH.pdb binding site in ICM-Pro. A shows riboflavin in the binding site, **B** shows lumichrome, **C** shows FMN, and **D** shows FAD. Green shading represents the hydrophobic region, blue shading represents the hydrogen bond acceptors, a white dashed arrow represents the hydrogen bonds, grey parabolas represent accessible surface for large areas, the broken thick line around the ligand shape indicates accessible surface, the size of the residue ellipse represents the strength of the contact, the 2D distance between the residue label and ligand represents proximity, and the covalently bound residue is represented with a thick black line around the ellipse.

Chapter 5

Discussion

Isothermal Titration Calorimetry

The results of ITC show that tight binding was associated with a more negative estimated binding energy value (ΔG^0) and smaller binding affinity value (K_d) (Table 4.1). According to ITC, riboflavin showed the highest affinity (tightest binding) to RBP of all the flavins, while FAD showed the lowest affinity to RBP (Table 4.1). From these results, it is hypothesized that the reason for the difference in the binding affinity values is a ligand-binding cleft. Figure 5.1 shows the riboflavin in the 4LRH.pdb cleft, which was measured by Wibowo et al. (2013) as ~10 × 15 Å with a depth of ~20 Å. For the riboflavin binding protein, the ligand-binding domain cleft was measured as ~20 Å wide and 15 Å deep, which accommodates the bound vitamin (riboflavin) (Monaco, 1997). The FAD and FMN are molecules with larger side chains off a three-ring structure – isoalloxazine. In the case of the two flavins, the side chains consist of two nucleotides and one nucleotide, respectively, compared to the side chain of riboflavin (Figure 4.1). The structural difference of FAD and FMN compared to riboflavin is hypothesized as the reason for their low affinity to RBP, especially since the cleft fits the riboflavin, vitamin B_2 (Monaco, 1997). Lumichrome, however, has only the basic three-ring structure and has no side chains compared to the other three flavins (Figure 4.1). The lumichrome binding affinity value was very close to riboflavin's value and thus lumichrome is able to fit into the cleft better than FAD and FMN, and, therefore, better able to bind with the active site without hindrance. The isoalloxazine ring was reported to be the most important contributor to the riboflavin tight binding to RBP (Choi and McCormick, 1980; Monaco, 1997). The fact that lumichrome's

structure is the isoalloxazine ring might explain why it had a closer binding affinity compared to riboflavin (Table 4.1).

ITC was more accurate than fluorescence spectrometry and ICM-Pro in measuring the binding affinity of the four flavins to RBP. When comparing the binding affinity results for the four flavins using ITC, ICM-Pro, and fluorescence spectrometry to the literature (Becvar and Plamer, 1982), ITC was shown to be the most similar. With regard to the riboflavin's binding affinity value, the ITC measurements were closer to the literature (Becvar and Palmer, 1982; Adiga, 1994; Nishikimi and Kyogoku, 1973) than ICM-Pro and fluorescence spectroscopy. What also confirms these results is the fact that the new generation of ITC is able to measure very accurate affinity binding (Freire et al., 1990).

Figure 5.1: Riboflavin in the binding pocket/cleft of 4LRH.pdb in ICM-Pro

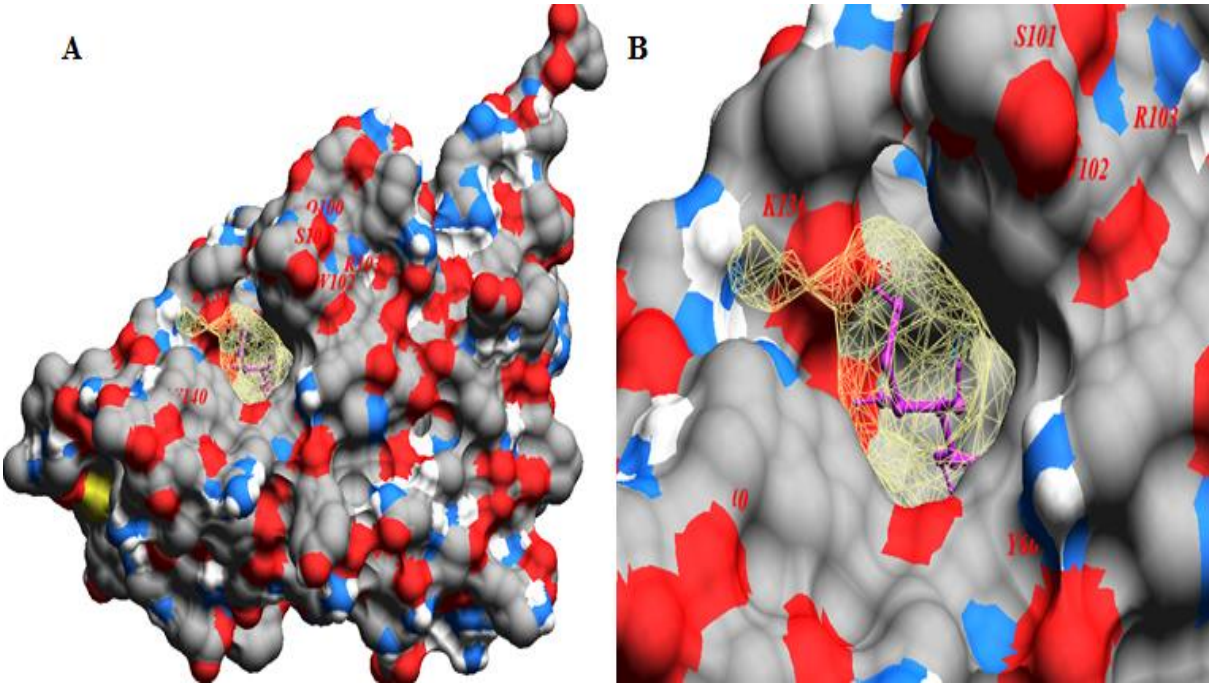

Riboflavin in the binding pocket/cleft of 4LRH.pdb in ICM-Pro. **A** shows the full view of the protein with riboflavin in the cleft and **B** shows a close-up view of the riboflavin in the protein's cleft.

Fluorescence Spectrometry

As in ITC, both the smaller K_d values and the more negative ΔG^0 values indicate tight affinity, and vice versa. The lumichrome had the highest affinity (tight) to RBP of all the flavins and FMN had the lowest affinity (Table 4.2).

The comparison of the flavins' binding affinity values (K_d) and calculated binding energy values (ΔG^0) from fluorescence spectroscopy with ITC was possible because variables such as temperature, pH, and buffer were controlled. When comparing the three flavins' K_d and ΔG^0 values between ITC and fluorescence spectrometry, a consistent difference is noticed. The K_d

average difference for the three flavins was calculated to be 4.735 M, and the ΔG^0 average difference was calculated to be 6.5 kcal/mole.

This consistent difference in values suggests that fluorescence spectrometry might be used as an inexpensive method to estimate the binding affinity of any flavin molecule to RBP. This process can be done by extrapolating the difference calculated in this research to other flavins to estimate their accurate binding affinity by only using fluorescence spectrometry. However, these experiments need to be repeated by using other flavins to determine if the difference is consistent between ITC and fluorescence spectrometry.

ICM-Pro

When using the computational program ICM-Pro, the results showed that the more negative estimated binding energy value (ΔG^0) resulted in a smaller calculated binding affinity value (K_d), thus demonstrating tighter binding. FAD showed the highest calculated affinity to 4LRH.pdb and lumichrome showed the lowest affinity (Table 4.3). The order of increased affinity matches the order of increased HBD and HBA numbers. Lumichrome showed the lowest number of HBD and HBA compared to the other flavins and had the lowest affinity to 4LRH.pdb. Similarly, the other three flavins are ordered in the same way with FAD having the highest affinity as well as the highest number of HBA and HBD.

When comparing K_d and ΔG^0 values for the four flavins between ITC and ICM-Pro, no consistent pattern is observed. However, drug-like molecules (riboflavin and lumichrome) had lower K_d and ΔG^0 values in ICM-Pro than in ITC. By contrast, nondrug-like molecules (FAD and FMN) had higher K_d and more negative ΔG^0 values in ICM-Pro than in ITC.

This discrepancy between ITC and ICM-Pro K_d and ΔG^0 values can possibly be explained by the following: ITC has many flavin molecules competing to bind to the RBP active site, whereas ICM-Pro had only one flavin molecule that was docked into the active site to computationally determine the estimated binding energy. ICM-Pro has demonstrated results similar to previous research (Ealy et al., 2017) where larger molecules such as FMN and FAD with a greater number of HBA and HBD bind more tightly because of increased possibilities of intermolecular attractions in the active site; it has not predicted accurate binding affinity as calculated from estimated binding energy.

As mentioned previously, ITC K_d and ΔG^0 values were observed to be associated with the size of the flavin molecules compared to riboflavin. The ICM-Pro results for the flavins were observed to be associated with the number of HBD and HBA for the flavins.

Sequence and Structural Similarities between RBP and 4LRH.PDB

Using BLAST, 4LRH.pdb was found to be the closest protein to RBP with 33% identity and 48% similarity. The E-value was 10^{-23}, which was small enough to indicate that this alignment had a very low possibility to have been by chance. Percent identity and E-value are important factors to be taken into when comparing two proteins. Any two proteins are considered homologous when approximately 30 % or higher of their sequences are identical, and the E-value of the alignment is far from 0 (negative direction) (Pearson, 2013; Johnson et al., 1994). This means that 4LRH.pdb and RBP are homologous, and they have a common evolutionary ancestry. The conservation of 16 cysteine amino acids that form 8 disulfide bonds has been reported previously (Monaco, 1997). The 72 shared hydrophobic amino acids, 89 shared polar

amino acids, and 17 shared aromatic amino acids show the extent of structural similarity RBP and 4LRH.pdb share.

The position of riboflavin in the RBP binding site (Monaco, 1997) is similar to its position in the 4LRH.pdb binding site. This similarity is specifically in regard to Tyr85 and Trp171 amino acids where the riboflavin xylene moiety is stacked between these two amino acids. The riboflavin xylene moiety was reported to have an essential role in the tight binding affinity of riboflavin to RBP (Monaco, 1997; Choi and McCromick, 1980). In addition, the distance of the Tyr85 and Trp171 planes from the riboflavin xylene plane in 4LRH.pdb is close to the distance values of the same amino acids in RBP (Monaco, 1997). The two amino acids are thought to contribute to hydrophobic, that is, π- π stacking interactions with riboflavin in 4LRH.pdb, which has been reported in RBP (Monaco, 1997).

Additionally, the four tryptophan amino acids that are located in the vicinity of each other in the 4LRH.pdb (Figure 4.19) binding site were also reported in the RBP active site (Figure 4.15) (Monaco, 1997). This observation also demonstrates how these aromatic amino acids might contribute to hydrophobic interactions in the binding site of both proteins. However, other amino acids that were in the RBP active site (Monaco, 1997) did not have corresponding amino acids in 4LRH.pdb. This observation might possibly explain the difference in the flavins' K_d and ΔG^0 values between ITC and ICM-Pro. On the other hand, the sequence and structural similarities between RBP and 4LRH.PDB are numerous.

Four amino acids (Ser57, Phe62, Trp134 and His135) in 4LRH.pdb were reported to form four hydrogen bonds with riboflavin (Figure 4.20). Our research suggests that four hydrogen bonds contribute to the estimated binding energy value of the riboflavin measured by ICM-Pro (Table 4.3). Figure 4.21 shows the hydrophobic interactions and hydrogen bonds of each of the

four flavins in the 4LRH.pdb binding site. These intermolecular interactions are important for understanding how the four flavins bind to the 4LRH.pdb binding site and how these interactions contribute to the estimated binding energy measurements.

Chapter 6

Conclusion

Significance of the Research and Future Work

The comparison of the four flavins' K_d and ΔG^0 between fluorescence spectrometry and ITC showed that based on the instrumentation used, fluorescence spectrometry was not an accurate method to measure the binding affinity. However, the consistent difference between the ITC and fluorescence spectrometry suggests that the latter could possibly be used to estimate the binding affinity for other flavins. Fluorescence spectrometry is a cheap method and can give results similar to those results obtained from ITC. The consistent difference in values has to be tested for many more flavins to verify the consistent difference. Future work can also do the same comparison for other flavin-like molecules to see if there is any consistency in differences between ITC and fluorescence spectrometry. If successful, money spent on the expensive ITC could be saved.

Although the comparison of the four flavins' K_d and ΔG^0 between ICM-Pro and ITC showed that ICM-Pro did not predict the accurate measurements produced by ITC, the results suggest that ICM-Pro's method of measuring the estimated binding energy did not account for the size of the active site protein cleft. There could also be other factors that ICM-Pro did not control for when measuring the estimated binding affinity of the flavins. However, future work is needed to test ICM-Pro in the calculation of the binding affinity from the estimated binding

energy. These tests could be done through measuring the binding affinity of the same flavins using ITC with human folate receptor alpha protein instead of RBP and then comparing the results to the current ICM-Pro results.

Previous research (Della-Longa and Arcovito, 2013) has compared the sequence and structure of human folate receptor alpha to riboflavin binding protein (RBP). This present research, however, was the first attempt to: 1) investigate the flavins' position in the active site of the folate receptor alpha 4LRH.pdb; 2) compare the riboflavin's position in the active site of 4LRH.pdb with its position in RBP (Monaco, 1997); 3) measure computationally the estimated binding energy and calculate the binding affinity of the flavins in the binding site of 4LRH.pdb; and 4) compare these values to the binding energies and binding affinities of the same four flavins in the RBP binding site using ITC. The results herein might provide new insights about the structural differences and similarities between RBP and the human folate receptor alpha protein. These insights could be beneficial in developing drugs for human folate receptor alpha that has been implicated in cancer (Cheung et al., 2016). These results would also be beneficial for future trials to develop cancer drugs against RBP because RBP has also been implicated in breast cancer (Rao et al., 1999). Further analysis of the interactions between flavins and human folate receptor alpha could also provide insights into the estimated binding energies obtained from ICM-Pro.

Limitations

The ITC experiments were not repeated for the four flavins. The reason was limited funding and time. The observed constant discrepancies between the fluorescence spectrometry

and ITC indicate some limitations in the spectrophotometer used. The spectrophotometer might not be able to accurately detect tight binding affinities, but was able to predict it with a difference in relation to the one obtained from ITC. Some of the flavins used were noticed to have precipitations when not stirred, which were determined by their solubility in the buffer used. The differences in solubility could affect the concentration of the flavins in the cuvette. Despite the effort to stir continuously, the possibility of inaccurate concentration still exists and could affect the K_d value. ITC uses changes in heat to measure affinity that might be more accurate than fluorescence spectrometry where the binding affinity is assessed from the quenching of the fluorescence by the protein.

FAD was not reported in fluorescence spectrometry because of limited time. Compared to the other flavins and early attempts to quench the fluorescence when using FAD, continuous addition of RBP would not quench the fluorescence. In addition, FAD fluorescence was barely detectable at high concentrations (10^{-3}M) and even at low concentrations (10^{-6}). Thus, finding the right FAD concentration that matches the other flavin concentrations and still show fluorescence on the spectrophotometer was challenging because of the limited time.

ICM-Pro's discrepancy in reporting the estimated binding energy compared to ITC is possibly because a different protein was used and, despite homology, it was unable to mimic the binding in the active site of RBP compared to the crystal structure of 4LRH.pdb that was used.

BIBLIOGRAPHY

Abagyan, R., Totrov, M., & Kuznetsov, D. (1994). ICM—a new method for protein modeling and design: applications to docking and structure prediction from the distorted native conformation. *Journal of Computational Chemistry, 15*(5), 488-506.

Adiga, P. R., Karande, A. A., Visweswariah, S. S., & Seshagiri, P. B. (1991). Carrier protein mediated transplacental riboflavin transport in the primate. *Perspectives in Primate Reproductive Biology*, 129-140.

Altschul, S.F., Gish, W., Miller, W., Myers, E.W. & Lipman, D.J. (1990). Basic local alignment search tool. *Journal of Molecular Biology, 215*:403-410.

Arnautova, Y. A., Abagyan, R. A., & Totrov, M. (2011). Development of a new physics-based internal coordinate mechanics force field and its application to protein loop modeling. *Proteins: Structure, Function, and Bioinformatics*, *79*(2), 477-498.

Bailey, L. B., & Gregory III, J. F. (1999). Folate metabolism and requirements. *The Journal of Nutrition, 129*(4), 779-782.

Becvar, J., & Palmer, G. (1982). The binding of flavin derivatives to the riboflavin-binding protein of egg white. A kinetic and thermodynamic study. *Journal of Biological Chemistry, 257*(10), 5607-5617.

Bell, I. R., Morrow, F. D., Read, M., Berkes, S., & Perrone, G. (1992). Low thyroxine levels in female psychiatric inpatients with riboflavin deficiency: implications for folate-dependent methylation. *Acta Psychiatrica Scandinavica, 85*(5), 360-363.

Benore-Parsons, M., Yonno, L., Mulholland, L., Saylor, W. W., & White, H. B. (1988). Transport of riboflavin-binding protein to the hen oocyte: Bound vitamin is not required for protein deposition. *Nutrition Research, 8*(7), 789-800.

Besaratinia, A., Kim, S. I., Bates, S. E., & Pfeifer, G. P. (2007). Riboflavin activated by ultraviolet A1 irradiation induces oxidative DNA damage-mediated mutations inhibited by vitamin C. *Proceedings of the National Academy of Sciences, 104*(14), 5953-5958.

Beveridge, D. L., & DiCapua, F. M. (1989). Free energy via molecular simulation: applications to chemical and biomolecular systems. *Annual Review of Biophysics and Biophysical Chemistry, 18*(1), 431-492.

Bolton, W. (1950). Free and combined riboflavin in the blood serum of estrogenized fowls. *Nature, 166*(4230), 912-913.

Chen, C., Ke, J., Zhou, X. E., Yi, W., Brunzelle, J. S., Li, J., ... & Melcher, K. (2013). Structural basis for molecular recognition of folic acid by folate receptors. *Nature, 500*, (7463), 486.

Chenprakhon, P., Sucharitakul, J., Panijpan, B., & Chaiyen, P. (2010). Measuring binding affinity of protein− ligand interaction using spectrophotometry: Binding of neutral red to riboflavin-binding protein. *Journal of Chemical Education*, *87*(8), 829-831.

Cheung, A., Bax, H. J., Josephs, D. H., Ilieva, K. M., Pellizzari, G., Opzoomer, J., ... & Canevari, S. (2016). Targeting folate receptor alpha for cancer treatment. *Oncotarget, 7*(32), 52553-52574.

Choi, J. D., & McCormick, D. B. (1980). The interaction of flavins with egg white riboflavin-binding protein. *Archives of Biochemistry and Biophysics*, *204*(1), 41-51.

Clarke, H. C. (1977). Distribution of riboflavin in blood: in women and in prenates. *International Journal for Vitamin and Nutrition Research, 47*(4), 361-363.

Common, R. H., Rutledge, W. A., & Bolton, W. (1946). The influence of gonadal hormones on serum riboflavin and certain other properties of blood and tissues in the domestic fowl. *Journal of Endocrinology, 5*(5), 121-130.

Cowan, J. W., Boucher, R. V., & Buss, E. G. (1966). Riboflavin utilization by a mutant strain of single comb white leghorn chickens: 3. riboflavin content of tissues. *Poultry Science, 45*(3), 536-538.

Dancis, J. (1962). The placenta in fetal nutrition and excretion. *American Journal of Obstetrics and Gynecology, 84*(11), 1749-1755.

Dancis, J., Lehanka, J., & Levitz, M. (1985). Transfer of riboflavin by the perfused human placenta. *Pediatric Research, 19*(11), 1143-1146.

Della-Longa, S., & Arcovito, A. (2013). Structural and functional insights on folate receptor α (FRα) by homology modeling, ligand docking and molecular dynamics. *Journal of Molecular Graphics and Modelling, 44*, 197-207.

DurgaKumari, B., & Adiga, P. R. (1986a). Hormonal induction of riboflavin carrier protein in the chicken oviduct and liver: a comparison of kinetics and modulation. *Molecular and Cellular Endocrinology, 44*(3), 285-292.

Durgakumari, B., & Adiga, P. (1986b). Estrogen modulation of retinol-binding protein in immature chicks: comparison with riboflavin carrier protein. *Molecular and Cellular Endocrinology, 46*(2), 121-130.

Ealy, J. B., Abouomar, N., Cogan, J., Flauta, P., Nassar, L., Mekolochik, M., ... & Yazgi, H. (2017). Estimated binding energies of drug-like and nondrug-like molecules in the active

site of HIV-1 Integrase, 1BIS. pdb, and two mutant models: Y143R and N155H. *Advances in Bioscience and Biotechnology*, *8*(05), 163-183.

Fenselau, C., Heller, D. N., Miller, M. S., & White, H. B. (1985). Phosphorylation sites in riboflavin-binding protein characterized by fast atom bombardment mass spectrometry. *Analytical Biochemistry*, *150*(2), 309-314.

Foy, H., & Kondi, A. (1953). A case of true red-cell aplastic anæmia successfully treated with riboflavin. *The Journal of Pathology*, *65*(2), 559-564.

Freire, E., Mayorga, O. L., & Straume, M. (1990). Isothermal titration calorimetry. *Analytical Chemistry*, *62*(18), 950A-959A.

Froehlich, J. A., Merrill, A. H., Clagett, C. O., & McCormick, D. B. (1980). Affinity chromatographic purification and comparison of riboflavin-binding proteins from laying hen liver and blood and from egg yolk. *Comparative Biochemistry and Physiology Part B: Comparative Biochemistry*, *66*(3), 397-401.

Gallicchio, E., & Levy, R. M. (2011). Recent theoretical and computational advances for modeling protein–ligand binding affinities. *Advances in Protein Chemistry and Structural Biology*, *85*, 27-80.

Goldsmith, G.A. (1975). Riboflavin Deficiency. In *Riboflavin* (pp. 221-244). Boston, MA: Springer.

Hamazume, Y., Mega, T., & Ikenaka, T. (1984). Characterization of hen egg-white and yolk-riboflavin binding proteins and amino acid sequence of egg white-riboflavin binding protein. *The Journal of Biochemistry*, *95*(6), 1633-1644.

Hamazume, Y., Mega, T. & Ikenaka, T. (1987). Position of disulfide bonds in riboflavin-binding protein of hen egg white. *The Journal of Biochemistry*, *101*, 217–223.

Hammer, C. H., Buss, E. G., & Clagett, C. O. (1973). Avian riboflavinuria: 8. the fate of the riboflavin-binding protein-riboflavin complex during incubation of hen's eggs. *Poultry Science, 52*(2), 520-530.

Innis, W. S., McCormick, D. B., & Merrill Jr, A. H. (1985). Variations in riboflavin binding by human plasma: identification of immunoglobulins as the major proteins responsible. *Biochemical Medicine, 34*(2), 151-165.

Johnson, T., Ouhtit, A., Gaur, R., Fernando, A., Schwarzenberger, P., Su, J., ... & Rao, P. (2009). Biochemical characterization of riboflavin carrier protein (RCP) in prostate cancer. *Frontiers Bioscience, 14*, 3634-3640.

Johnson, M. S., Srinivasan, N., Sowdhamini, R., & Blundell, T. L. (1994). Knowledge-based protein modeling. *Critical Reviews in Biochemistry and Molecular Biology*, *29*(1), 1-68.

Jorgensen, W. L. (2004). The many roles of computation in drug discovery. *Science, 303*(5665), 1813-1818.

Jusko, W. J., & Levy, G. (1969). Plasma protein binding of riboflavin and riboflavin-*5′*-phosphate in Man. *Journal of Pharmaceutical Sciences*, *58*(1), 58-62.

Kane, M. A., Elwood, P. C., Portillo, R. M., Antony, A. C., Najfeld, V., Finley, A., ... & Kolhouse, J. F. (1988). Influence on immunoreactive folate-binding proteins of extracellular folate concentration in cultured human cells. *The Journal of Clinical Investigation, 81*(5), 1398-1406.

Kaaks, R., Tuyns, A. J., Haelterman, M., & Riboli, E. (1998). Nutrient intake patterns and gastric cancer risk: A case-control study in Belgium. *International Journal of Cancer, 78*(4), 415-420.

Karande, A. A., Sridhar, L., Gopinath, K. S., & Adiga, P. R. (2001). Riboflavin carrier protein: a serum and tissue marker for breast carcinoma. *International Journal of Cancer, 95*(5), 277-281.

Kelemen, L. E. (2006). The role of folate receptor α in cancer development, progression and treatment: cause, consequence or innocent bystander? *International Journal of Cancer, 119*(2), 243-250.

Kim, R., & Skolnick, J. (2008). Assessment of programs for ligand binding affinity prediction. *Journal of Computational Chemistry, 29*(8), 1316-1331.

Kudle, K. R., Kudle, M. R., Merugu, R., & Rudra, M. P. (2017). Purification and characterization of riboflavin carrier protein from guinea pig serum and cytotoxic activity of its antisera against Hela cancer cells. *Journal of Chemical and Pharmaceutical Sciences (JCPS), 10*(2), 923-928.

Kuriyan, J., Konforti, B., & Wemmer, D. (2009). Molecular recognition: The thermodynamics of binding. In *The Molecules of Life: Physical and Chemical Principles* (pp. 531-580). New York: Garland Science.

Kurplus, M., & McCammon, J. A. (1983). Dynamics of proteins: elements and function. *Annual Review of Biochemistry, 52*(1), 263-300.

Mason, C. W., D'Souza, V. M., Bareford, L. M., Phelps, M. A., Ray, A., & Swaan, P. W. (2006). Recognition, cointernalization, and recycling of an avian riboflavin carrier protein in human placental trophoblasts. *Journal of Pharmacology and Experimental Therapeutics, 317*(2), 465-472.

McCormick, D. B., Innis, W.S.A., Merrill, A. H., Jr., Bowers-Komro, D. M., Oka, M. & Chastain, J. L. (1988). An update on flavin metabolism in rats and humans. In *Flavins and Flavoproteins* (pp. 459–471). New York: Walter de Gruyter.

Merrill, A. H., & Mccormick, D. B. (1978). Flavin affinity chromatography: General methods for purification of proteins that bind riboflavin. *Analytical Biochemistry, 89*(1), 87-102.

Merrill, A. H., Jr., Shapira, G. & McCormick, D. B. (1982). Recent findings concerning mammalian riboflavin-binding proteins. In *Flavins and Flavoproteins* (pp. 508–513). New York: Elsevier Biomedical.

Mifflin, T. E., & Langerman, N. (1983). Calorimetric studies of flavin binding protein: Flavin analog binding. *Archives of Biochemistry and Biophysics, 224*(1), 319-325.

Miller, M.S., Benore-Parsons, M. and White, H.B., III (1982a). Dephosphorylation of chicken riboflavin-binding protein and phosphovitin decreases their uptake by oocytes. *Journal of Biological Chemistry, 257*, 6818–6824.

Miller, M. S., Bruch, R. C., & White, H. B. (1982b). Carbohydrate compositional effects on tissue distribution of chicken riboflavin-binding protein. *Biochimica et Biophysica Acta (BBA) - General Subjects, 715*(1), 126-136.

Miller, M. S., Buss, E. G., & Clagett, C. O. (1981). Effect of carbohydrate modification on transport of chicken egg white riboflavin-binding protein. *Comparative Biochemistry and Physiology Part B: Comparative Biochemistry*, *69*(4), 681-686.

Monaco HL (1997) Crystal structure of chicken riboflavin-binding protein. *The EMBO Journal, 16*:1475–1483.

Morris, H. P. (1947). Effects on the genesis and growth of tumors associated with vitamin intake. *Annals of the New York Academy of Sciences, 49*(1), 119-140.

Morris, H. P., & Robertson, W. V. B. (1943). Growth rate and number of spontaneous mammary carcinomas and riboflavin concentration of liver, muscle, and tumor of C3H mice as influenced by dietary riboflavin. *Journal of the National Cancer Institute*, *3*(5), 479-489.

Motulsky, H. J. One site -- Specific binding, GraphPad Curve Fitting Guide. Accessed April 01, 2018, http://www.graphpad.com/guides/prism/7/curve-fitting/index.htm?reg_standard_errors_and_confidence.htm

Murthy, U. S., & Adiga, P. R. (1978a). Estrogen-induced synthesis of riboflavin-binding protein in immature chicks kinetics and hormonal specificity. *Biochimica et Biophysica Acta (BBA)-General Subjects, 538*(2), 364-375.

Murthy, U. S., & Adiga, P. R. (1978b). Oestrogen induction of riboflavin-binding protein in immature chicks. Nature of the secretory protein. *Biochemical Journal*, *170*(2), 331-335.

Murthy, U. S., Sreekrishna, K., & Adiga, P. R. (1979). A simplified method for the purification of riboflavin-binding protein from hen's egg yolk. *Analytical Biochemistry, 92*(2), 345-350.

Murty, C. R., & Adiga, P. R. (1981). Mechanism of foetal wastage following immunoneutralisation of riboflavin carrier protein in the pregnant rat. *FEBS Letters, 135*(2), 281-284.

Natraj, U., George, S., & Kadam, P. (1988). Isolation and partial characterisation of human riboflavin carrier protein and the estimation of its levels during human pregnancy. *Journal of Reproductive Immunology, 13*(1), 1-16.

Natraj, U., Kumar R, A., & Kadam, P. (1987). Termination of pregnancy in mice with antiserum to chicken riboflavin-carrier protein. *Biology of Reproduction, 36*(3), 677-685.

Nishikimi, M., & Kyogoku, Y. (1973). Flavin-protein interaction in egg white flavoprotein. *The Journal of Biochemistry, 73*(6), 1233-1242.

Norioka, N., Okada, T., Hamazume, Y., Mega, T., & Ikenaka, T. (1985). Comparison of the amino acid sequences of hen plasma-, yolk-, and white-riboflavin binding proteins. *The Journal of Biochemistry, 97*(1), 19-28.

Pearson, W. R. (2013). An Introduction to Sequence Similarity ("Homology") Searching. *Current Protocols in Bioinformatics / Editoral Board, Andreas D. Baxevanis ... [et Al.]*. Chapter 3. Unit3.1. 10.1002/0471250953.bi0301s42.

Pollard, T. D. (2010). A guide to simple and informative binding assays. *Molecular Biology of the Cell, 21*(23), 4061-4067.

Powers, H. J. (2003). Riboflavin (vitamin B-2) and health. *The American Journal of Clinical Nutrition, 77*(6), 1352-1360.

Rao, P. N., Crippin, J., Levine, E., Hunt, J., Baliga, S., Balart, L., ... & Raj, M. H. (2006). Elevation of serum riboflavin carrier protein in hepatocellular carcinoma. *Hepatology Research, 35*(2), 83-87.

Rao, P. N., Levine, E., Myers, M. O., Prakash, V., Watson, J., Stolier, A., ... & Raj, M. H. (1999). Elevation of serum riboflavin carrier protein in breast cancer. *Cancer Epidemiology and Prevention Biomarkers, 8*(11), 985-990.

Rhodes, M. B., Bennett, N., & Feeney, R. E. (1959). The flavoprotein-apoprotein system of egg white. *Journal of Biological Chemistry, 234*, 2054-2060.

Siassi, F., & Ghadirian, P. (2005). Riboflavin deficiency and esophageal cancer: a case control-household study in the Caspian Littoral of Iran. *Cancer Detection and Prevention, 29*(5), 464-469.

Squires, M. W., & Naber, E. C. (1992). Vitamin profiles of eggs as indicators of nutritional status in the laying hen: vitamin B12 study 1, 2. *Poultry Science, 71*(12), 2075-2082.

Stover, P. J. (2004). Physiology of folate and vitamin B 12 in health and disease. *Nutrition Reviews, 62*(suppl_1), S3-S12.

Subramanian, S., & Adiga, P. R. (1999). Immunological relatedness of chicken and human riboflavin carrier protein. *Biochemical and Biophysical Research Communications, 262*(2), 539-544.

Tsao, S. M., Yin, M. C., & Liu, W. H. (2007). Oxidant stress and B vitamins status in patients with non-small cell lung cancer. *Nutrition and Cancer, 59*(1), 8-13.

Vaidya, S. M., Kamlakar, P. L., & Kamble, S. M. (1998). Molybdenum, xanthine oxidase and riboflavin levels in tamoxifen treated postmenopausal women with breast cancer. *Indian Journal of Medical Sciences, 52*(6), 244-247.

Visweswariah, S. S., & Adiga, P. R. (1987a). Isolation of riboflavin carrier proteins from pregnant human and umbilical cord serum: similarities with chicken egg riboflavin carrier protein. *Bioscience Reports, 7*(7), 563-571.

Visweswariah, S. S., & Adiga, P. R. (1987b). Purification of a circulatory riboflavin carrier protein from pregnant bonnet monkey (M. radiata): comparison with chicken egg vitamin carrier. *Biochimica et Biophysica Acta (BBA)-Protein Structure and Molecular Enzymology, 915*(2), 141-148.

Warkany, J., & Nelson, R. C. (1942). Congenital malformations induced in rats by maternal nutritional deficiency. *Journal of Nutrition, 23*, 321-333.

White III, H. B. (1987). Vitamin-binding proteins in the nutrition of the avian embryo. *The Journal of Experimental Zoology, 1*, 53-63.

White III, H. B., & Merrill Jr, A. H. (1988). Riboflavin-binding proteins. *Annual Review of Nutrition, 8*(1), 279-299.

White, H. B., Nuwaysir, E. F., Komara, S. P., Anderson, D. A., Chang, S. J., Sherwood, T. A., ... & Saylor, W. W. (1992). Effect of riboflavin-binding protein deficiency on riboflavin metabolism in the laying hen. *Archives of Biochemistry and Biophysics, 295*(1), 29-34.

Wibowo, A. S., Singh, M., Reeder, K. M., Carter, J. J., Kovach, A. R., Meng, W., ... & Dann, C. E. (2013). Structures of human folate receptors reveal biological trafficking states and diversity in folate and antifolate recognition. *Proceedings of the National Academy of Sciences*, *110*(38), 15180-15188.

Winter, W. P., Buss, E. G., Clagett, C. O., & Boucher, R. V. (1967). The nature of the biochemical lesion in avian renal riboflavinuria—II. The inherited change of a riboflavin-binding protein from blood and eggs. *Comparative Biochemistry and Physiology, 22*(3), 897-906.

Yamashita, K., Kamerling, J. P., & Kobata, A. (1983). Structural studies of the sugar chains of hen ovomucoid. Evidence indicating that they are formed mainly by the alternate biosynthetic pathway of asparagine-linked sugar chains. *Journal of Biological Chemistry, 258*(5), 3099-3106.

Yang, H. T., Chao, P. C., & Yin, M. C. (2013). Riboflavin at high doses enhances lung cancer cell proliferation, invasion, and migration. *Journal of Food Science*, *78*(2), 343-349.

Zak, Z., & Ostrowski, W. (1963). Preparation and properties of riboflavin flavoprotein of soluble fraction of egg yolk. *Acta Biochimica Polonica, 10*, 427-441.

Zak, Z., Ostrowski, W., Steczko, J., Weber, M., Gizler, M., & Morawiecki, A. (1972). Riboflavin carrier protein from egg yolk. Spectral and other properties observed upon binding of flavin to apoprotein. *Acta Biochimica Polonica, 19*(4), 307-323.

Zhang, X., Tworoger, S. S., Eliassen, A. H., & Hankinson, S. E. (2013). Postmenopausal plasma sex hormone levels and breast cancer risk over 20 years of follow-up. *Breast Cancer Research and Treatment, 137*(3), 883-892.

Zheng, D. B., Lim, H. M., Pene, J. J., & White, H. B. (1988). Chicken riboflavin-binding protein. cDNA sequence and homology with milk folate-binding protein. *Journal of Biological Chemistry, 263*(23), 11126-11129.

Zschäbitz, S., Cheng, T. Y. D., Neuhouser, M. L., Zheng, Y., Ray, R. M., Miller, J. W., ... & Shikany, J. M. (2013). B vitamin intakes and incidence of colorectal cancer: results from the Women's Health Initiative Observational Study cohort. *The American Journal of Clinical Nutrition, 97*(2), 332-343.

Academic Vita of Habib Yazgi
Yazgi.habib@gmail.com

EDUCATION

The Pennsylvania State University, Schreyer Honors College
Degree: B.S. Honors in Biology

THESIS TITLE: Binding Affinities of Flavins to Riboflavin Binding Protein using Fluorescence Spectrometry and Isothermal Titration Calorimetry, and Estimated Binding Energies using Computational Approaches.
THESIS SUPERVISOR: Julie Ealy

HONORS & AWARDS:

Freshman President Award.	2015
Renaissance Scholarship	2015-2016
Trustee Scholarship	2015-2016
Outstanding Student in Biology Award	2016
Bioinorganic Workshop Grant	2016
Batdorf Trustee Scholarship	2016-2017
Boscov Honors Program Scholarship	2016-2017
Renaissance Fund Scholarship	2016-2017
Wagner Renaissance Scholarship Lehigh Valley	2016-2017
Internal Scholarship: Schreyer Honors College	2016-2017
The Evan Pugh Scholar Award	2017
Kappa Phi Kappa Honors Society	2017
Lindquist Family Trustee Scholarship (Schreyer Honors College)	2017-2018
Dean's List	2014-2018

PUBLICATIONS

Yazgi, H., Cogan, J. W., Atashpanjeh, S., McLaughlin, J. S. (2016). The Effects of Bovine Serum on the Growth Dynamics of A10 Cells in Culture. *The Journal of Introductory Biology Investigation*, *3*(5), 1-7.

Ealy, J.B., Abouomar, N., Cogan, J., Flauta, P., Nassar, L., Mekolochik, M., Ramzy, S., Shannon, C., Nassar, and **Yazgi, H.** (2017). Estimated Binding Energies of Drug-Like and Nondrug-Like Molecules in the Active Site of HIV-1 Integrase, 1BIS.pdb, and Two Mutant Models: Y143R and N155H. *Advances in Bioscience and Biotechnology*, *8*, 163-183.

PRESENTATIONS

Yazgi, H.; Abouomar, N.; Cogan, J.; Ealy, J. B. Estimated Binding Energies of Drug-like and Nondrug-like Molecules in the Active Site of HIV-1 Integrase, 1BIS.pdb, and Mutated 1BIS.pdb. 8/21/2016. American Chemical Society meeting, Philadelphia, PA.

Yazgi, H.; Abouomar, N.; Ealy, J. B. Spectrophotometric Fluorescence and Isothermal Titration Calorimetry Used to Determine the Binding Affinity of Flavins with Riboflavin Binding Protein and Computationally Calculated Estimated Binding Energy. 6/5/2017. Middle Atlantic Regional Meeting of the American Chemical Society, Hershey, PA.

COMMUNITY SERVICE INVOLVEMENT

Radiology Department at St. Luke Hospital, Allentown	2016-2017
Emergency Department at St. Luke Hospital, Allentown	Summer 2017
Red Cross at Allentown, PA	2017-2018

LANGUAGE PROFICIENCY

Arabic (Native)
English
French